

Supplement to: Climate model Selection by Independence, Performance, and Spread (ClimSIPS) for regional applications

Anna L. Merrifield¹, Lukas Brunner², Ruth Lorenz¹, Vincent Humphrey¹, and Reto Knutti¹

¹Institute for Atmospheric and Climate Science, ETH Zurich, Zurich, Switzerland

²Department of Meteorology and Geophysics, University of Vienna, Vienna, Austria

Correspondence: Anna L. Merrifield (anna.merrifield@env.ethz.ch)

This supplement includes Tables, Figures, and Text to support the main text and is structured as follows:

1. **CMIP Ensemble:** Text S1, Tables S1 to S3,
2. **Model Dependence:** Text S2, Table S4, Figures S1 to S4
3. **Effective Equilibrium Climate Sensitivity (ECS) in the literature:** Text S3, Figure S5
5. **Model Performance:** Text S4, Figure S6 to S10
5. **Model Spread:** Text S5, Figure S11 to S13
6. **ClimSIPS:** Text S6, Tables S5 and S6, Figure S14

1 CMIP Ensembles

Supplementary Tables S1 to S3 provide additional information about the CMIP6 and CMIP5 ensembles used in this study,
10 including members used and references. The "Members Used" column lists all members used in Section 3 (Revisiting Model
Dependence) of the main text, while the "Case Study Member(s)?" column indicates which members are then used in Section
5 (ClimSIPS for European climate applications) of the main text.

2 Model Independence

Model dependence is established by an optimal "fingerprint" that consists of global temperature and pressure climatologies
15 masked by between-model spread / internal variability thresholds. The CMIP6 fingerprint (and its component masks) are shown
in the main text; the CMIP5 fingerprint is shown in Supplementary Figure S1. The between-model spread mask is defined by
the standard deviation across CMIP5/6 "one member per model" ensembles. The CMIP5 one member per model ensemble
consists of member "r1i1p1" from each of the 29 uniquely named models. The CMIP6 one member per model ensemble, listed

in Supplementary Table S4, is comprised of member "r1i1p1f1" when available. Exceptions include "r1i1p1f2" for UKESM1-0-LL, CNRM-CM6-1-HR, CNRM-ESM2-1, CNRM-CM6-1, MIROC-ES2L, and MCM-UA-1-0, "r1i1p1f3" for HadGEM3-GC31-MM and HadGEM3-GC31-LL, and "r1i1p3f1" for GISS-E2-1-G. The internal variability mask is defined as the median of standard deviations (σ) in 12 CMIP6 initial condition ensembles and five CMIP5 initial condition ensembles. With standard deviations shown in Supplementary Figure S2 for the global SAT field and Supplementary Figure S3 for the global SLP field, initial condition ensembles used are made up of five or more ensemble members. The 12 CMIP6 ensembles are:

- 25 1. ACCESS-ESM1-5, r(1-10)i1p1f1
 2. CanESM5, r(1-25)i1p1f1
 3. CESM2, r(1,2,4,10,11)i1p1f1
 4. CNRM-CM6-1, r(1-6)i1p1f2
 5. CNRM-ESM2-1, r1i1p1f2
30 6. EC-Earth3, r(1,3,4,6,9,11,13,15)i1p1f1
 7. GISS-E2-1-G, r(1-5)i1p3f1
 8. IPSL-CM6A-LR, r(1-4,6,14)i1p1f1
 9. MIROC-ES2L, r(1-10)i1p1f2
 10. MIROC6, r(1-50)i1p1f1
35 11. MPI-ESM1-2-LR, r(1-10)i1p1f1
 12. UKESM1-0-LL, r(1-4,8)i1p1f2

The five CMIP5 ensembles are:

- 40 1. CanESM2, r(1-5)i1p1
 2. CCSM4, r(1-6)i1p1
 3. CNRM-CM5, r(1,2,4,6,10)i1p1
 4. CSIRO-Mk3-6-0, r(1-10)i1p1
 5. EC-EARTH, r(1,2,8,9,12)i1p1

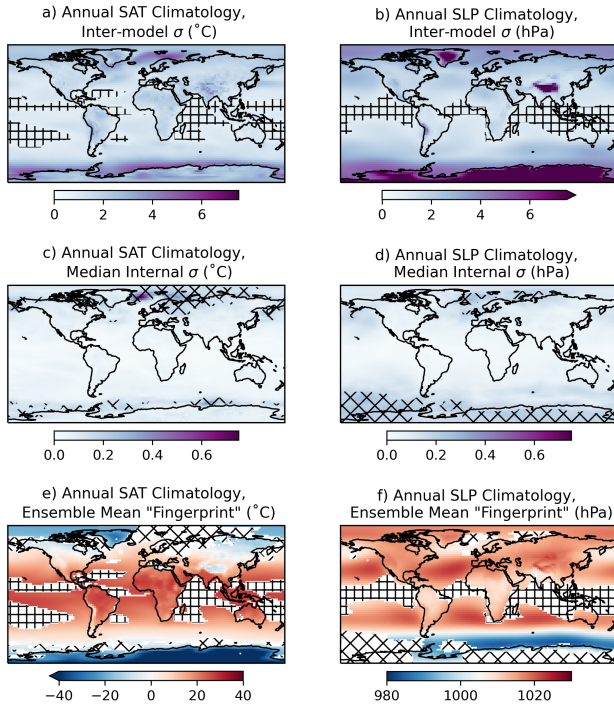


Figure S1. Determining the spatial "fingerprint" within the fields used to identify CMIP5 climate model dependence: annual mean SAT ($^{\circ}\text{C}$) and SLP (hPa) climatology averaged over the period 1905–2005. (a,b) a measure of between-model spread of the dependence predictors, computed as the standard deviation (σ) across a one member per model CMIP5 ensemble comprised of r1i1p1 simulations. Square hatching indicates where between-model spread is low, at or below its 15th percentile. (c,d) Median internal variability of the dependence predictors, computed as the median of the standard deviations within the five CMIP5 initial condition ensembles with five or more members (CanESM2, CCSM4, CNRM-CM5, CSIRO-Mk3-6-0, and EC-EARTH). Diamond hatching indicates where median internal variability is high, at or above its 85th percentile. (e,f) Fingerprint used to determine dependence, shown as the ensemble mean climatology of the whole CMIP5 ensemble with the regions of low between-model spread and high internal variability masked and hatched with square and diamond hatching respectively.

Additionally, we considered global annually-averaged precipitation climatology for use as a predictor to define model families. The precipitation fingerprint is shown in Supplementary Figure S4 for CMIP5/6. The predictor was not used in the model dependence definition because the region of elevated between-model spread (important for ensuring models are distinguishable from one another) coincides with and is therefore masked by the region of elevated internal variability (important for grouping known dependencies). Therefore, the predictor does not add value to the overall dependence definition because un-masked regions are similar amongst all models.

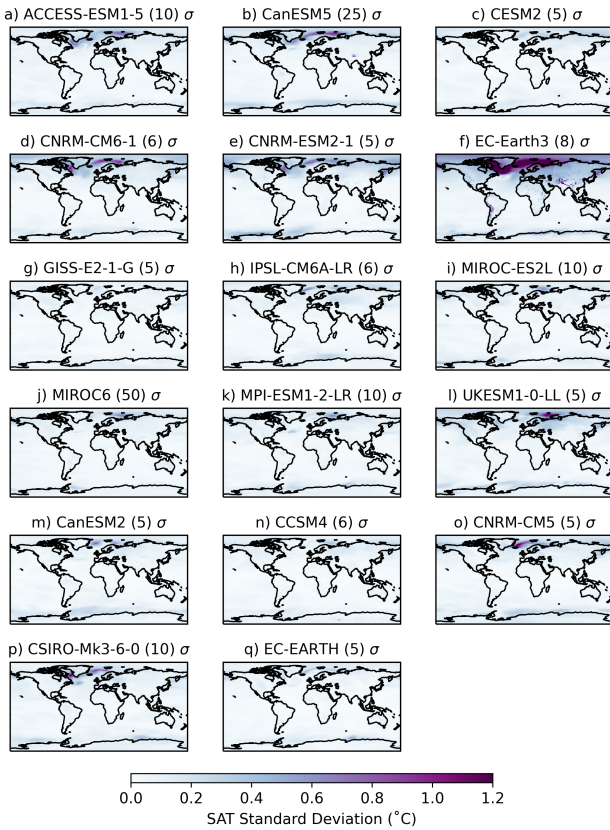


Figure S2. Internal variability of Annual Average Surface Air Temperature Climatology (1905-2005) represented by the standard deviation (σ) across members of initial condition ensembles with five or more members within CMIP6 (a-l) and CMIP5 (m-q). The number of members in each ensemble is listed in parentheses in each title.

3 Effective Equilibrium Climate Sensitivity (ECS) in the literature

50 Supplementary Figure S5 compiles effective equilibrium climate sensitivity (ECS) values from CMIP5/6 models reported in recent literature. All values were reported to be calculated using the Gregory et al. (2004) method, through a (halved) linear fit of the net top-of-atmosphere radiance vs. surface temperature curve in the first 150 years of a simulation with an atmospheric CO₂ concentration that has been instantaneous quadrupled. We compile CMIP5/6 ECS values from 12 sources, listed below and in the legend of Sup. Fig. S5. Differences between reported values are not always clearly traceable, but where a potential explanation exists, it is noted below:

1. Meehl et al. (2020): Values rounded to the tenths place rather than the hundredths place.
2. Seland et al. (2020a)
3. Nijssse et al. (2020): Mean values are reported for models with multiple realizations.

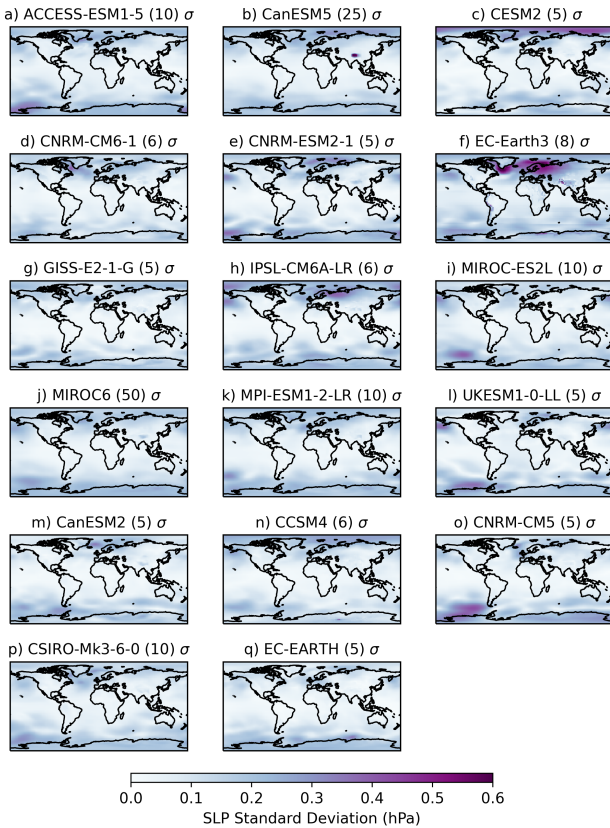


Figure S3. As in Figure S2, but for Annual Average Sea Level Pressure Climatology (1905-2005).

- 4. Flynn and Mauritsen (2020)
- 60 5. Golaz et al. (2019)
- 6. Bacmeister et al. (2020): Value rounded to the tenths place rather than the hundredths place.
- 7. Schlund et al. (2020)
- 8. Zelinka et al. (2020): Values are given for "flagship" model variants, typically (but not always) the "r1i1p1" or "r1i1p1f1" simulation for CMIP5 and CMIP6, respectively.
- 65 9. Tokarska et al. (2020)
- 10. Pak et al. (2021)
- 11. Wyser et al. (2020)

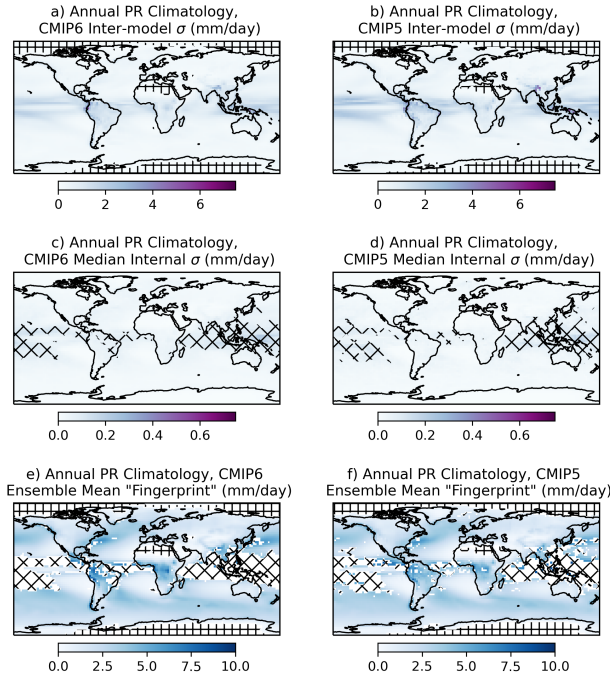


Figure S4. The spatial fingerprint of annual mean PR (mm/day) climatology averaged over the period 1905-2005. (a,b) Between-model spread of the precipitation field in CMIP6 and CMIP5 respectively. Square hatching indicates where between-model spread is low, at or below its 15th percentile. (c,d) Median internal variability of the precipitation fields within the twelve CMIP6 and five CMIP5 initial condition ensembles with five or more members. Diamond hatching indicates where median internal variability is high, at or above its 85th percentile. (e,f) Precipitation fingerprint shown as the ensemble mean climatology of the whole CMIP6 and CMIP5 ensembles with the regions of low between-model spread and high internal variability masked and hatched with square and diamond hatching respectively.

12. Smith et al. (2021): Values reported in the IPCC's Assessment Report 6 Working Group I Chapter 7 Supplementary Material (The Earth's energy budget, climate feedbacks, and climate sensitivity) Table 7.SM.5.
- 70 In the main text, we use the ECS values reported by the IPCC (Smith et al., 2021) if available. Additional sources for CMIP6 include Zelinka et al. (2020) [CMCC-ESM2, EC-Earth3, GFDL-CM4, and GFDL-ESM4], Golaz et al. (2019) [E3SM-1-1], and Pak et al. (2021) [KIOST-ESM]. Additional sources for CMIP5 include Bacmeister et al. (2020) [CESM1-CAM5], Wyser et al. (2020) [EC-EARTH], and Selander et al. (2020a) [NorESM1-ME].

4 Model Performance

- 75 We employ ClimSIPS for Central European (CEU) Summer (JJA) applications and Northern European (NEU) Winter (DJF) applications in both the CMIP6 and CMIP5 ensembles. Model performance is one of three dimensions on which models can

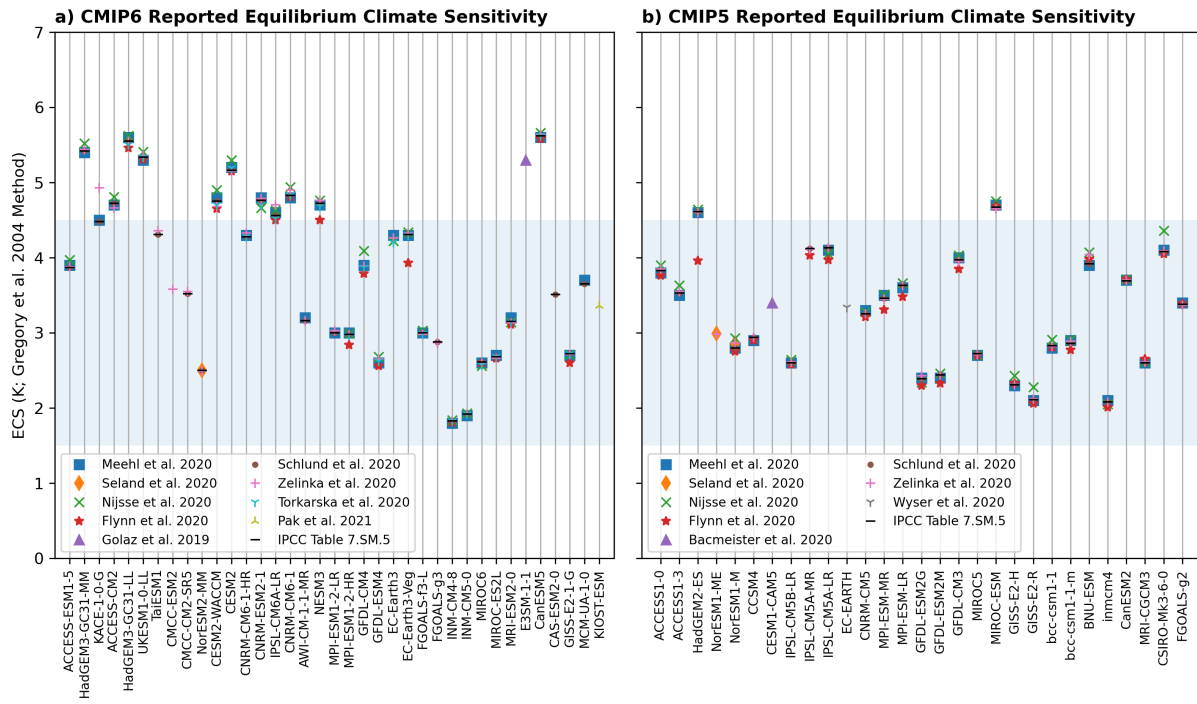


Figure S5. a) CMIP6 and b) CMIP5 Effective Equilibrium Climate Sensitivity (ECS) values reported in recent research (legend). The Charney et al. (1979) range of uncertainty (1.5 to 4.5°C) is shaded in blue. ECS is calculated using the method described in Gregory et al. (2004).

be selected. In the European case studies, model performance is defined by six predictors, four that comprise an annual base set and two that are seasonally relevant.

Predictors in the annual base set are:

- 80 – Annual-average ocean masked European ($30^{\circ} - 76.25^{\circ}\text{N}$, $10^{\circ}\text{E} - 39^{\circ}\text{W}$) SAT climatology; 1950-1969
- Annual-average ocean masked European ($30^{\circ} - 76.25^{\circ}\text{N}$, $10^{\circ}\text{E} - 39^{\circ}\text{W}$) SAT climatology; 1995-2014
- Annual-average North Atlantic ($37^{\circ} - 60^{\circ}\text{N}$, $50^{\circ} - 15^{\circ}\text{E}$) sea surface temperature (SST) climatology; 1995-2014
- Annual-average Southern Hemisphere midlatitude ($30^{\circ} - 60^{\circ}\text{S}$) shortwave cloud radiative effect (SWCRE) climatology; 2001-2018

85 Additional predictors used for JJA CEU applications are:

- JJA average Central Europe Station PR climatology; 1995-2014 - masked by the union of the CEU SREX mask (Iturbide et al., 2020) and the E-OBS dataset mask (Cornes et al., 2018)
- JJA average CEU SWCRE climatology; 2001-2018

Additional predictors used for DJF NEU applications are:

- 90 – DJF average Northern Europe Station PR climatology; 1995-2014 - masked by the union of the NEU SREX mask
(Iturbide et al., 2020) and the E-OBS dataset mask (Cornes et al., 2018)
- DJF average North Atlantic Sector ($25^{\circ} - 73^{\circ}\text{N}$, $42^{\circ}\text{E}-20^{\circ}\text{W}$) SLP climatology; 1950-2014

For each individual predictor, performance is determined by the root-mean-square error (RMSE) between model and observed fields (Supplementary Figures S6-S9, a-f). Overall performance (Sup. Figs. S6-S9, g) is the average of the six individual predictor RMSEs. In Sup. Figs. S6-S9, individual predictor or aggregated performance is plotted against "changes of interest": midcentury, regional European temperature or precipitation change for the CMIP5 (blue x's) and CMIP6 (orange o's) simulations listed in Supplementary Tables S1-S3.

A summary of model performance for the European case studies explored in this study is presented in Supplementary Figure S10. Models are ordered from highest performer to lowest performer by (where applicable) ensemble mean performance (Sup. Fig. S10, stars) or individual member performance (Sup. Fig. S10, horizontal lines).

5 Model Spread

Along with model performance, model spread is another of three dimensions on which models can be selected. As stated in the main text, spread is defined as:

$$S_{ij} = \sqrt{(\text{SAT}\Delta_i - \text{SAT}\Delta_j)^2 + (\text{PR}\Delta_i - \text{PR}\Delta_j)^2} \quad (1)$$

105 with $\text{SAT}\Delta$ and $\text{PR}\Delta$ representing normalized change in SAT and PR between 2041-2060 and 1995-2014 mean states.

SAT and PR change within CMIP be defined by ensemble mean or by individual member. Within CMIP, models can be represented by a single simulation or by an ensemble of simulations. For models represented by a single simulation, SAT and PR change are fixed. For models represented by multiple ensemble members, SAT and PR change could reflect the average of all ensemble members or the value of any individual ensemble member. These two options are shown in Figure 12a,b in the main text for CMIP6 JJA CEU applications and in Supplementary Figure S12 for CMIP5 JJA CEU applications, Supplementary Figure S11 for CMIP6 DJF NEU applications, and Supplementary Figure S13 for CMIP5 DJF NEU applications.

Using a strategy analogous to the KKZ algorithm (Katsavounidis et al., 1994) discussed in the main text, individual members are chosen from each model ensemble in order to maximize ensemble spread. The following models are represented by a single simulation and were placed first.

- 115 – CMIP6: AWI-CM-1-1-MR-r1i1p1f1, CMCC-CM2-SR5-r1i1p1f1, CMCC-ESM2-r1i1p1f1, CNRM-CM6-1-HR-r1i1p1f2, E3SM-1-1-r1i1p1f1, FGOALS-f3-L-r1i1p1f1, GFDL-CM4-r1i1p1f1, GFDL-ESM4-r1i1p1f1, GISS-E2-1-G-r1i1p3f1, INM-CM4-8-r1i1p1f1, INM-CM5-0-r1i1p1f1, KIOST-ESM-r1i1p1f1, NorESM2-MM-r1i1p1f1, and TaiESM1-r1i1p1f1.

**Predictor RMSE from Observed vs. JJA Central European SAT Change
(2041/2060 - 1995/2014)**

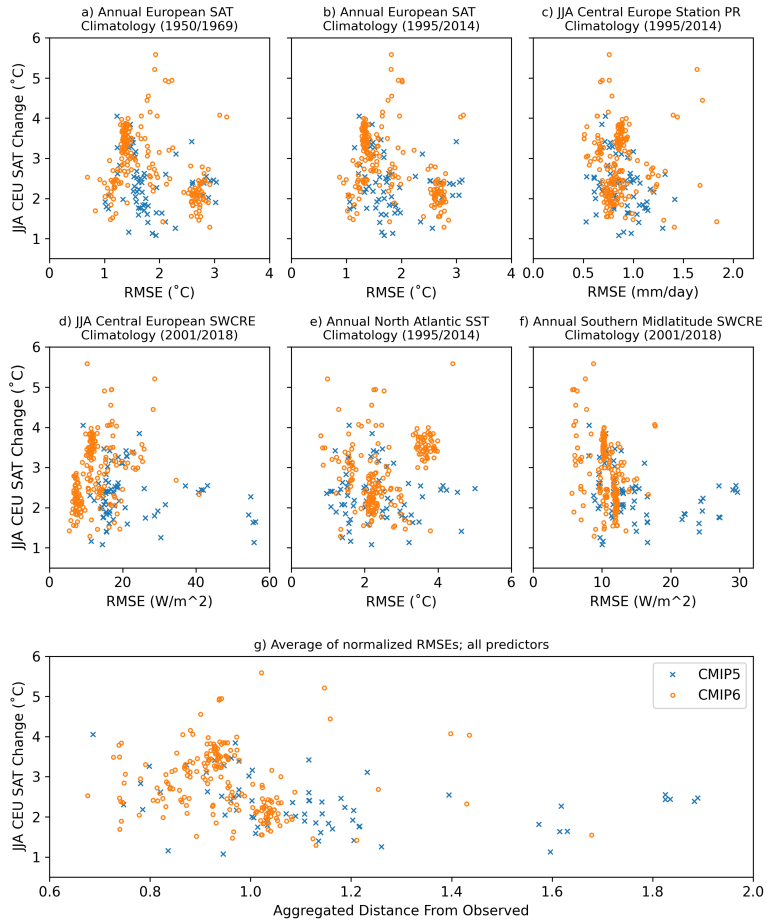


Figure S6. Root mean square error (RMSE) between observed and predictor fields scattered against JJA Central European SAT Change ($^{\circ}\text{C}$) between 2041-2060 and 1995-2014 for each member of the CMIP6 SSP5-8.5 (orange) and CMIP5 (blue) RCP8.5 ensembles. Relationships with individual predictors are shown in panels a through f and the relationship between the aggregate distance from observations, computed as the average of the individual predictor RMSEs normalized by their respective combined CMIP5 and CMIP6 ensemble mean value is shown in panel g.

- CMIP5: ACCESS1-0-r1i1p1, ACCESS1-3-r1i1p1, GFDL-CM3-r1i1p1, GFDL-ESM2G-r1i1p1, GFDL-ESM2M-r1i1p1, IPSL-CM5A-MR-r1i1p1, IPSL-CM5B-LR-r1i1p1, MIROC-ESM-r1i1p1, MPI-ESM-MR-r1i1p1, MRI-CGCM3-r1i1p1, NorESM1-M-r1i1p1, NorESM1-ME-r1i1p1, bcc-csm1-1-m-r1i1p1, bcc-csm1-1-r1i1p1, and inmcm4-r1i1p1

120 Members were then selected from the remaining model ensembles in the following order.

**Predictor RMSE from Observed vs. JJA Central European PR Change
(2041/2060 - 1995/2014)**

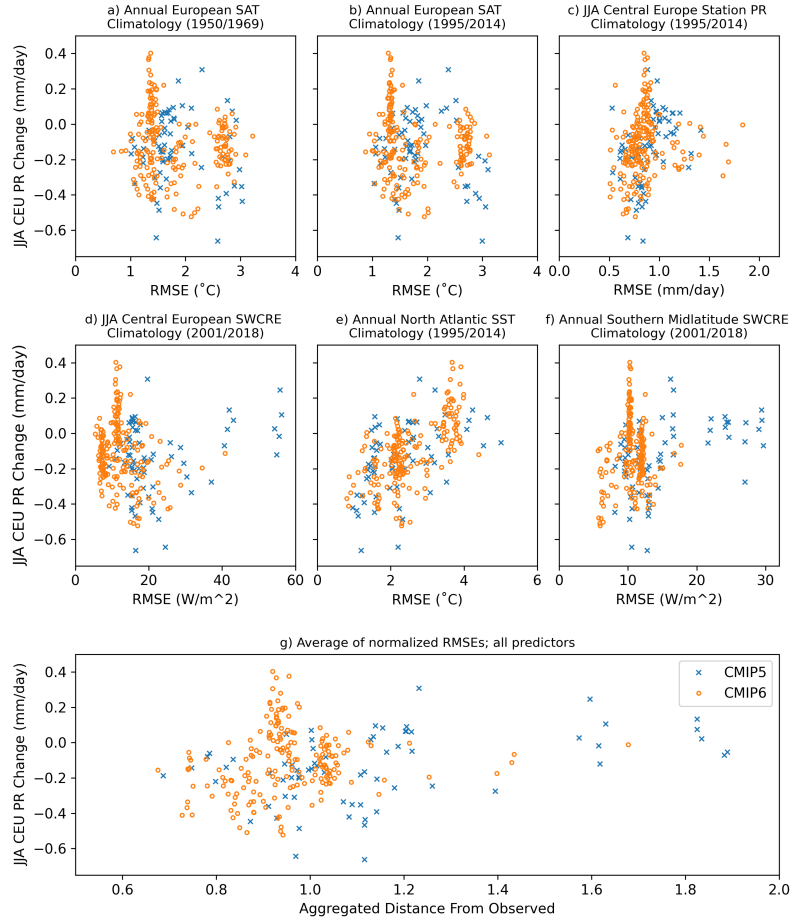


Figure S7. As in Figure S6, but with RMSEs scattered against JJA Central European PR Change (mm/day) between 2041-2060 and 1995-2014.

- CMIP6: ACCESS-CM2, ACCESS-ESM1-5, CAS-ESM2-0, CESM2-WACCM, CESM2, CNRM-CM6-1, CNRM-ESM2-1, CanESM5, FGOALS-g3, HadGEM3-GC31-LL, HadGEM3-GC31-MM, IPSL-CM6A-LR, KACE-1-0-G, MIROC-ES2L, MIROC6, MPI-ESM1-2-HR, MPI-ESM1-2-LR, MRI-ESM2-0, NESM3, UKESM1-0-LL
- 125 – CMIP5: CCSM4, CESM1-CAM5, CNRM-CM5, CSIRO-Mk3-6-0, CanESM2, GISS-E2-H, GISS-E2-R, HadGEM2-ES, IPSL-CM5A-LR, MIROC5, MPI-ESM-LR

**Predictor RMSE from Observed vs. DJF Northern European SAT Change
(2041/2060 - 1995/2014)**

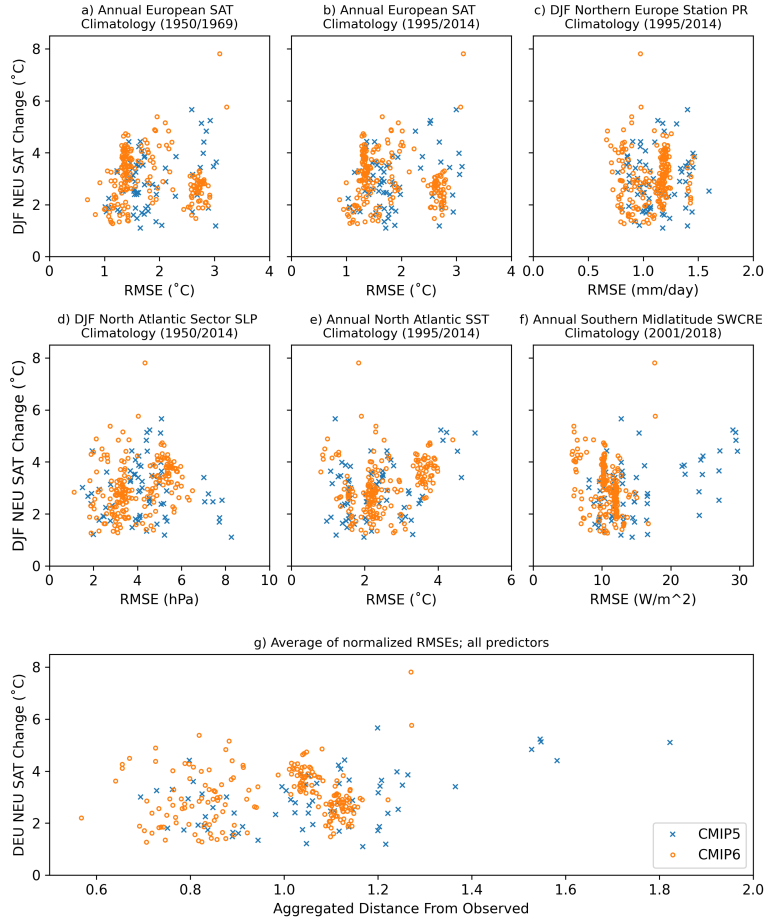


Figure S8. As in Figure S6, but with DJF NEU predictor RMSEs scattered against DJF Northern European SAT Change ($^{\circ}\text{C}$) between 2041-2060 and 1995-2014.

Several other selection orders were also evaluated. We find that selection order tends to affect which member is selected from 1-3 model ensembles but does not substantially change the overall individual member SAT-PR change distribution.

6 ClimSIPS

- 130 To accompany the ternary selection triangles in the main text, we provide a quick reference of recommended model subsets and an example of cost function individual component magnitudes. Recommended model subsets are listed in Supplementary

**Predictor RMSE from Observed vs. DJF Northern European PR Change
(2041/2060 - 1995/2014)**

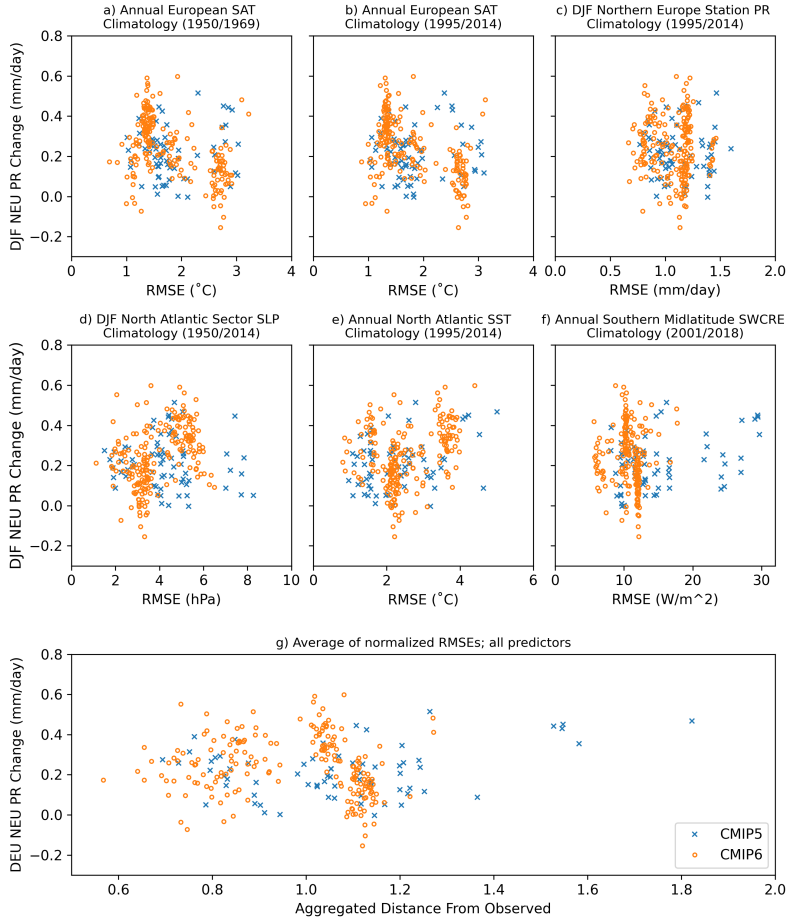


Figure S9. As in Figure S6, but with DJF NEU predictor RMSEs scattered against DJF Northern European PR Change (mm/day) between 2041-2060 and 1995-2014.

Tables S5 and S6. Each recommended subset is listed with the relative importance of performance, independence, and spread based on the median α and β for which the subset minimizes the cost function.

Supplementary Figure S14 accompanies the CMIP6 JJA CEU 34 choose 3 subselections, shown in Figures 8 and 9 of the main text. Shown are the performance, independence, and spread components that minimize the subselection cost function:

$$C_{\alpha,\beta}(s_1, \dots, s_n) = (1 - \alpha - \beta) \cdot P(s_1, \dots, s_n) - \alpha \cdot I(s_1, \dots, s_n) - \beta \cdot S(s_1, \dots, s_n) \quad (2)$$

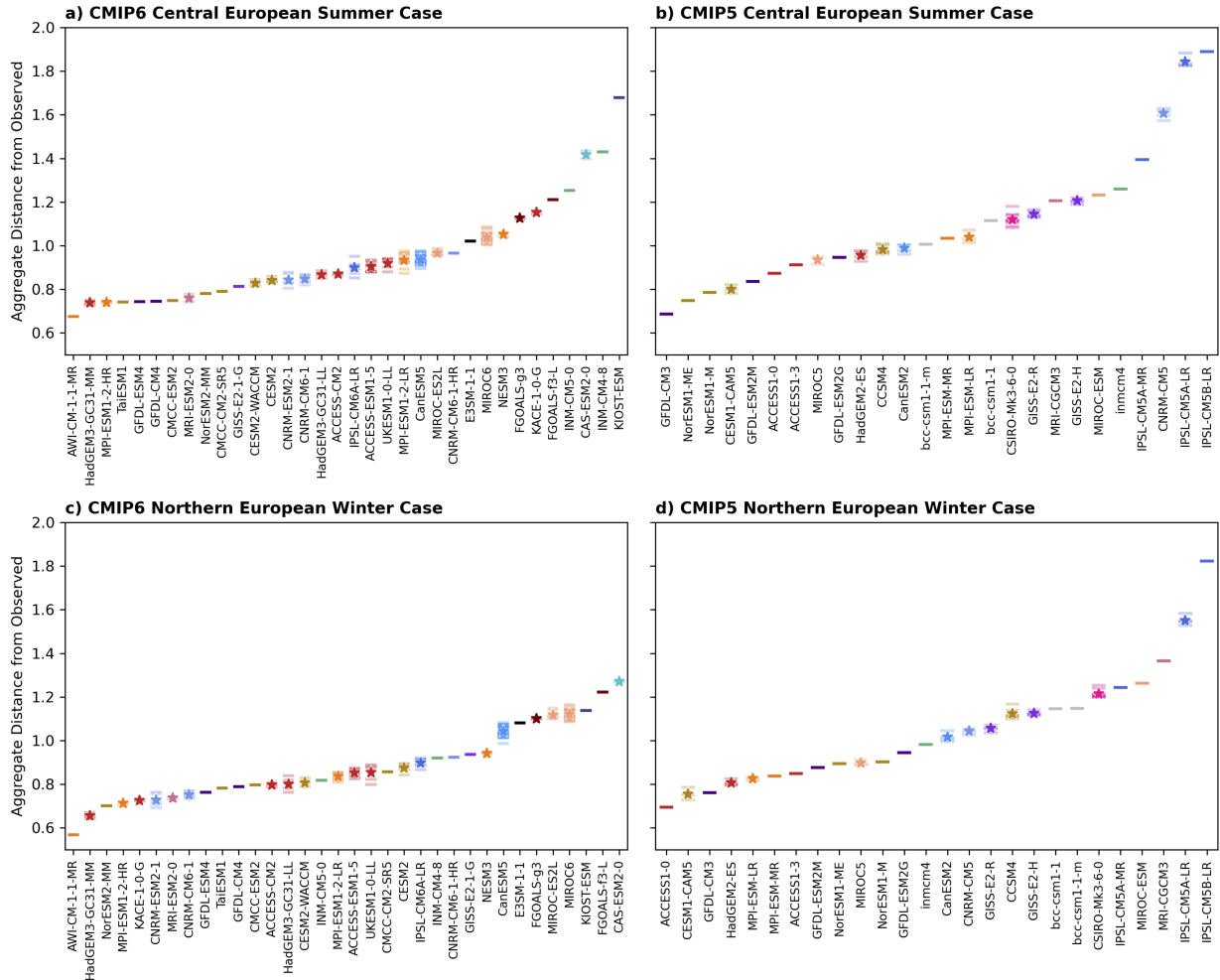


Figure S10. CMIP6 and CMIP5 models ordered by aggregated distance from observed, a metric based on the average of model-observed RMSE for the six predictors chosen for Central European Summer (panels a and b, respectively) or Northern European Winter applications (panels c and d, respectively). Performance order, with higher performers closer to observed, is based on ensemble mean performance where applicable, i.e. when a model is represented by more than one ensemble member. Horizontal lines represent the performance of individual ensemble members while stars indicate ensemble mean performance. Note that performance order differs in the two cases.

for each α and β when models are represented by ensemble mean (Sup. Fig. S14a-c) and when models are represented by individual spread-maximizing member (Sup. Fig. S14d-f). Because $P(s_1, \dots, s_n)$, $I(s_1, \dots, s_n)$, and $S(s_1, \dots, s_n)$ are normalized, they are unitless; component magnitudes relate to the distributions of the three considerations. In terms of sign, components 140 are shown in accordance with the sign in the cost function. $P(s_1, \dots, s_n)$, shown in Sup. Fig. S14a,d, maintains its positive sign; negative values of $P(s_1, \dots, s_n)$ occur in subsets comprised of models with below-average aggregated distance from observations

CMIP6 Northern European Winter Case

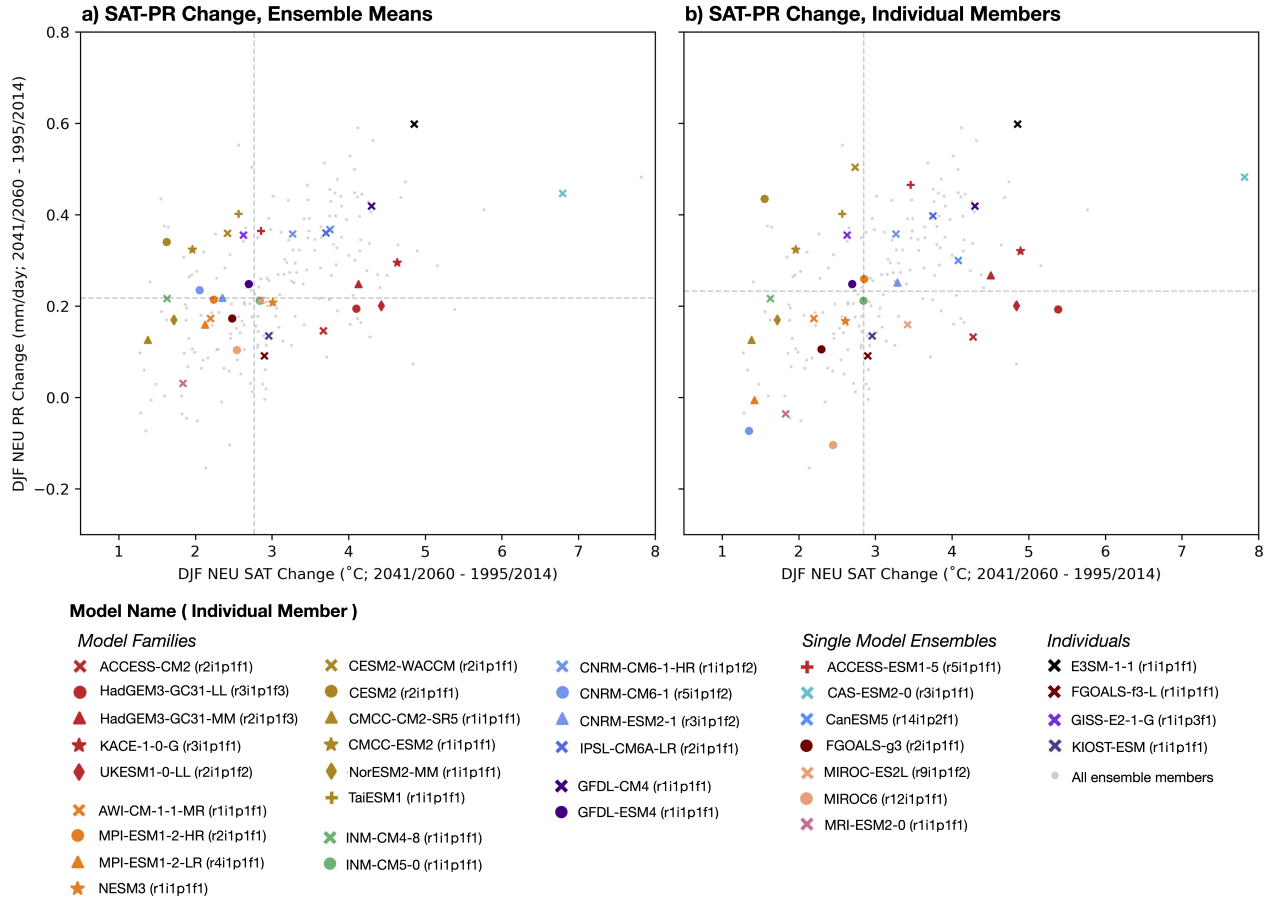


Figure S11. As in Figure 9a,b from the main text, but for CMIP6 DJF NEU applications. Ensemble means (colored markers) are shown in panel a in DJF NEU SAT and PR change space (note: not normalized) superposed on all ensemble members (light gray dots). Individual ensemble members, shown in panel b and labeled in parentheses, were selected to maximize spread. In both panels, ensemble median values for DJF NEU SAT and PR change (gray dashed lines) delineate the four quadrants used for spread recommendations.

(corresponding to above-average performance). $I(s_1, \dots, s_n)$ (Sup. Fig. S14b,e) and $S(s_1, \dots, s_n)$ (Sup. Fig. S14c,f) are negated; negative values in these panels reflect subsets comprised of models with above average independence or spread.

CMIP5 Central European Summer Case

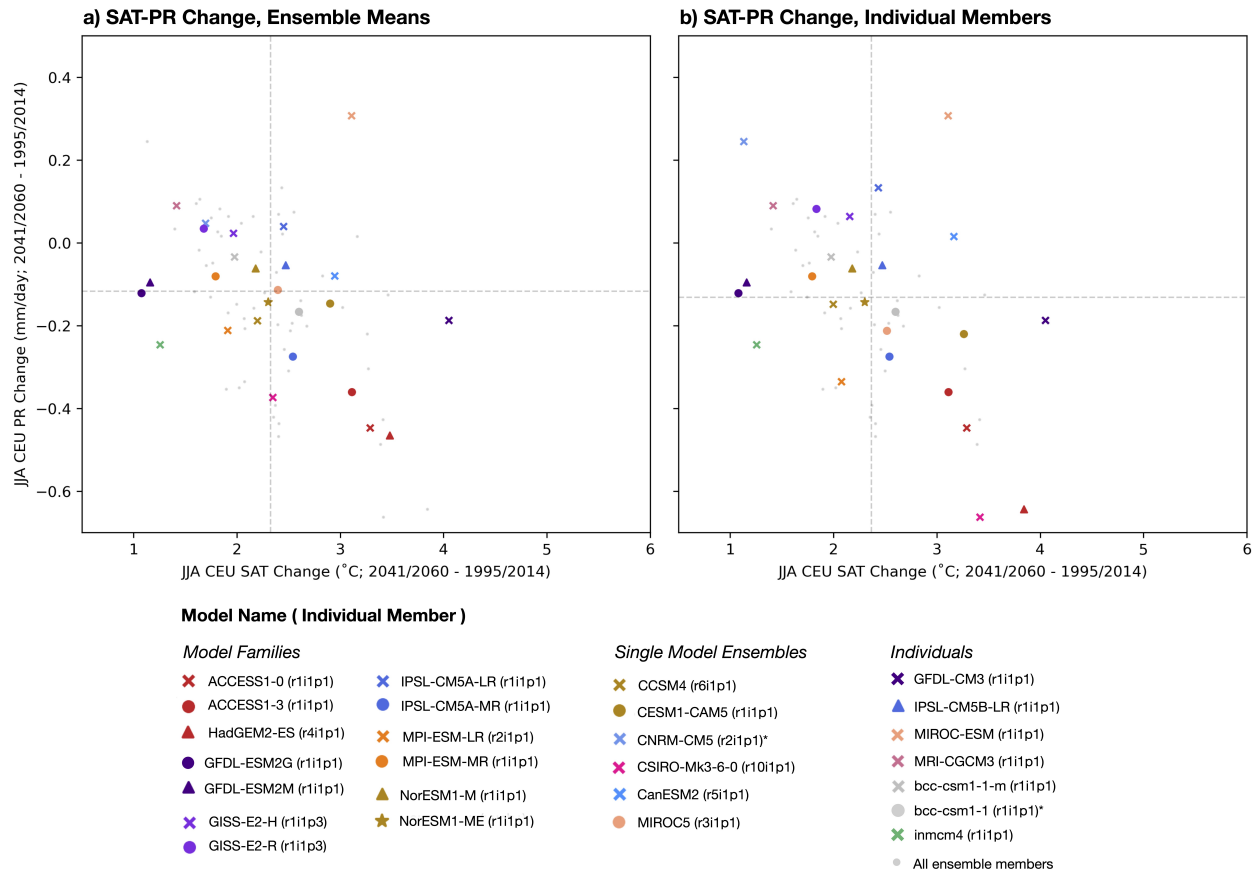


Figure S12. As in Figure S11, but for CMIP5 JJA CEU applications. Models with starred labels, CNRM-CM5 and bcc-csm1-1, fall in a different family designation than in the main text due to family members lacking the performance predictor fields required for inclusion into the case study.

References

- 145 Andrews, M. B., Ridley, J. K., Wood, R. A., Andrews, T., Blockley, E. W., Booth, B., Burke, E., Dittus, A. J., Florek, P., Gray, L. J., Haddad, S., Hardiman, S. C., Hermanson, L., Hodson, D., Hogan, E., Jones, G. S., Knight, J. R., Kuhlbrodt, T., Misios, S., Mizielinski, M. S., Ringer, M. A., Robson, J., and Sutton, R. T.: Historical Simulations With HadGEM3-GC3.1 for CMIP6, Journal of Advances in Modeling Earth Systems, 12, e2019MS001995, <https://doi.org/10.1029/2019MS001995>, 2020.
- Bacmeister, J. T., Hannay, C., Medeiros, B., Gettelman, A., Neale, R., Fredriksen, H. B., Lipscomb, W. H., Simpson, I., Bailey, D. A., Holland, M., Lindsay, K., and Otto-Btiesner, B.: CO₂ Increase Experiments Using the CESM: Relationship to Climate Sensitivity and Comparison of CESM1 to CESM2, Journal of Advances in Modeling Earth Systems, 12, e2020MS002120, <https://doi.org/10.1029/2020MS002120>, 2020.

CMIP5 Northern European Winter Case

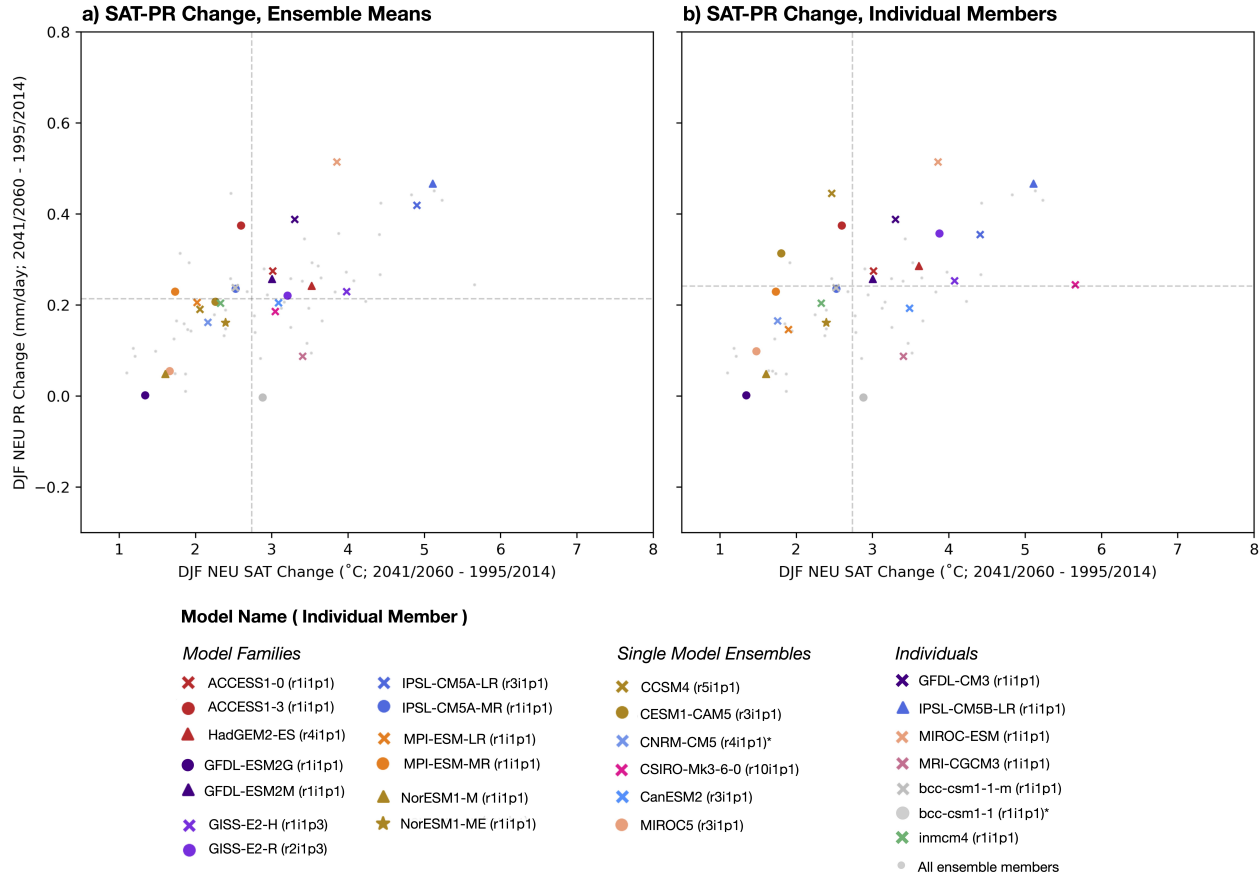


Figure S13. As in Figure S11 and S12 , but for CMIP5 DJF NEU applications. Models with starred labels, CNRM-CM5 and bcc-csm1-1, fall in a different family designation than in the main text due to family members lacking the performance predictor fields required for inclusion into the case study.

Bentsen, M., Bethke, I., Debernard, J. B., Iversen, T., Kirkevåg, A., Seland, Ø., Drange, H., Roelandt, C., Seierstad, I. A., Hoose, C., and Kristjánsson, J. E.: The Norwegian Earth System Model, NorESM1-M – Part 1: Description and basic evaluation of the physical climate, 155 Geoscientific Model Development, 6, 687–720, <https://doi.org/10.5194/gmd-6-687-2013>, 2013.

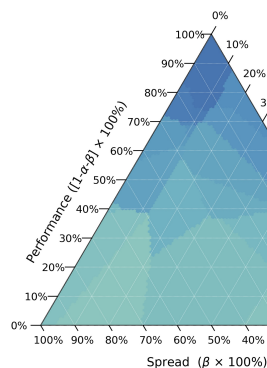
Bi, D., Dix, M., Marsland, S., O'Farrell, S., Rashid, H., Uotila, P., Hirst, Kowalczyk, E., Golebiewski, Sullivan, A., Yan, Y., Hannah, Franklin, C., Sun, Z., Vohralik, Watterson, Fiedler, R., Collier, M., and Puri, K.: The ACCESS coupled model: Description, control climate and evaluation, Australian Meteorological and Oceanographic Journal, 63, 41–64, <https://doi.org/10.22499/2.6301.004>, 2012.

Bi, D., Dix, M., Marsland, S., O'Farrell, S., Sullivan, A., Bodman, R., Law, R., Harman, I., Jhan, S., Rashid, H., Dobrohotoff, P., Chloe, M., 160 Hailin, Y., Tony, H., Savita, A., Dias, F., Fiedler, R., and Heerdegen, A.: Configuration and spin-up of ACCESS-CM2, the new generation Australian Community Climate and Earth System Simulator Coupled Model, Journal of Southern Hemisphere Earth System Science, 70, <https://doi.org/10.1071/ES19040>, 2020.

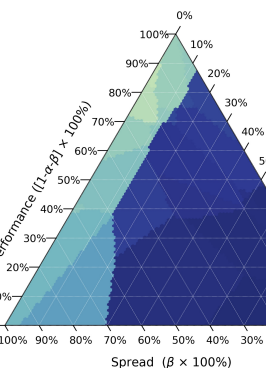
CMIP6 Central European Summer Case

3 Model Subselection by Ensemble Mean

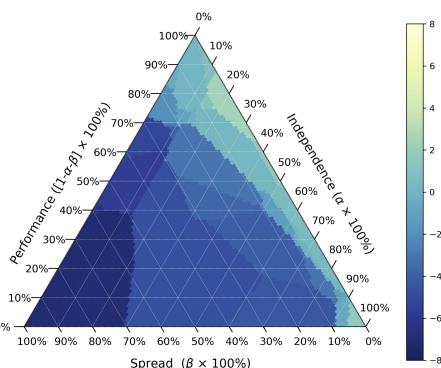
a) Performance Component of Minimized Cost Function



b) Independence Component of Minimized Cost Function

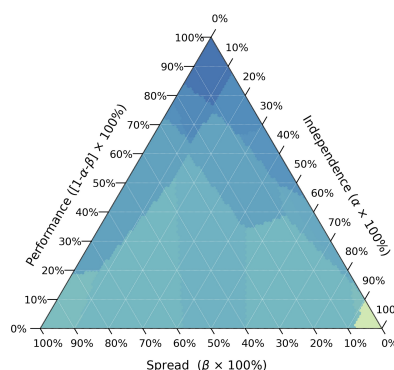


c) Spread Component of Minimized Cost Function

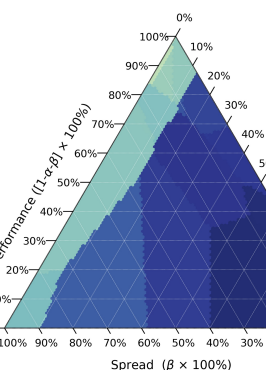


3 Model Subselection by Individual Member

d) Performance Component of Minimized Cost Function



e) Independence Component of Minimized Cost Function



f) Spread Component of Minimized Cost Function

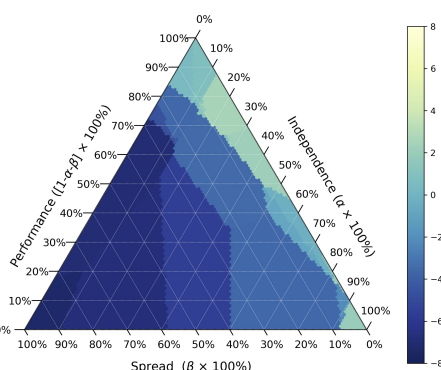


Figure S14. A comparison of performance, independence, and spread components of the minimized cost function that selects model sets from the full CMIP6 ensemble for JJA CEU applications. Panels a-c show the components for 3 model subselection by ensemble means (as shown in main text Figure 8) and panels d-f show the components for 3 model subselection by individual member (as shown in main text Figure 9). The components are presented with the respective sign of each term (positive for performance, negative for independence and spread), such that to compute the value of the minimized cost function, the three component values are multiplied by $(1-\alpha-\beta)$, α , or β , respectively and summed.

Boucher, O., Servonnat, J., Albright, A. L., Aumont, O., Balkanski, Y., Bastrikov, V., Bekki, S., Bonnet, R., Bony, S., Bopp, L., Braconnot, P., Brockmann, P., Cadule, P., Caubel, A., Cheruy, F., Codron, F., Cozic, A., Cugnet, D., D'Andrea, F., Davini, P., de Lavergne, C., Denvil, S., Deshayes, J., Devilliers, M., Ducharne, A., Dufresne, J.-L., Dupont, E., Éthé, C., Fairhead, L., Falletti, L., Flavoni, S., Foujols, M.-A., Gardoll, S., Gastineau, G., Ghosh, J., Grandpeix, J.-Y., Guenet, B., Guez, Lionel, E., Guiyadi, E., Guimbarteau, M., Hauglustaine, D., Hourdin, F., Idelkadi, A., Joussaume, S., Kageyama, M., Khodri, M., Krinner, G., Lebas, N., Levavasseur, G., Lévy, C., Li, L., Lott, F., Lurton, T., Luyssaert, S., Madec, G., Madeleine, J.-B., Maignan, F., Marchand, M., Marti, O., Mellul, L., Meurdosoif, Y., Mignot, J., Musat,

- I., Ottlé, C., Peylin, P., Planton, Y., Polcher, J., Rio, C., Rochetin, N., Rousset, C., Sepulchre, P., Sima, A., Swingedouw, D., Thiéblemont, 170 R., Traore, A. K., Vancoppenolle, M., Vial, J., Vialard, J., Viovy, N., and Vuichard, N.: Presentation and Evaluation of the IPSL-CM6A-LR Climate Model, *Journal of Advances in Modeling Earth Systems*, 12, e2019MS002 010, <https://doi.org/10.1029/2019MS002010>, 2020.
- Cao, J., Wang, B., Yang, Y.-M., Ma, L., Li, J., Sun, B., Bao, Y., He, J., Zhou, X., and Wu, L.: The NUIST Earth System Model (NESM) version 3: description and preliminary evaluation, *Geoscientific Model Development*, 11, 2975–2993, <https://doi.org/10.5194/gmd-11-2975-2018>, 2018.
- 175 Charney, J. G., Arakawa, A., Baker, D. J., Bolin, B., Dickinson, R. E., Goody, R. M., Leith, C. E., Stommel, H. M., and Wunsch, C. I.: Carbon dioxide and climate: A scientific assessment, National Academy of Sciences, Washington, D. C., 1979.
- Cherchi, A., Fogli, P. G., Lovato, T., Peano, D., Iovino, D., Gualdi, S., Masina, S., Scoccimarro, E., Materia, S., Bellucci, A., and Navarra, A.: Global Mean Climate and Main Patterns of Variability in the CMCC-CM2 Coupled Model, *Journal of Advances in Modeling Earth Systems*, 11, 185–209, <https://doi.org/10.1029/2018MS001369>, 2019.
- 180 Cornes, R. C., van der Schrier, G., van den Besselaar, E. J. M., and Jones, P. D.: An Ensemble Version of the E-OBS Temperature and Precipitation Data Sets, *Journal of Geophysical Research: Atmospheres*, 123, 9391–9409, <https://doi.org/10.1029/2017JD028200>, 2018.
- Danabasoglu, G., Lamarque, J.-F., Bacmeister, J., Bailey, D. A., DuVivier, A. K., Edwards, J., Emmons, L. K., Fasullo, J., Garcia, R., Gettelman, A., Hannay, C., Holland, M. M., Large, W. G., Lauritzen, P. H., Lawrence, D. M., Lenaerts, J. T. M., Lindsay, K., Lipscomb, W. H., Mills, M. J., Neale, R., Oleson, K. W., Otto-Bliesner, B., Phillips, A. S., Sacks, W., Tilmes, S., van Kampenhout, L., Vertenstein, M., Bertini, A., Dennis, J., Deser, C., Fischer, C., Fox-Kemper, B., Kay, J. E., Kinnison, D., Kushner, P. J., Larson, V. E., Long, M. C., Mickelson, S., Moore, J. K., Nienhouse, E., Polvani, L., Rasch, P. J., and Strand, W. G.: The Community Earth System Model Version 2 (CESM2), *Journal of Advances in Modeling Earth Systems*, 12, e2019MS001 916, <https://doi.org/10.1029/2019MS001916>, 2020.
- 185 Donner, L. J., Wyman, B. L., Hemler, R. S., Horowitz, L. W., Ming, Y., Zhao, M., Golaz, J.-C., Ginoux, P., Lin, S.-J., Schwarzkopf, M. D., Austin, J., Alaka, G., Cooke, W. F., Delworth, T. L., Freidenreich, S. M., Gordon, C. T., Griffies, S. M., Held, I. M., Hurlin, W. J., Klein, S. A., Knutson, T. R., Langenhorst, A. R., Lee, H.-C., Lin, Y., Magi, B. I., Malyshev, S. L., Milly, P. C. D., Naik, V., Nath, M. J., Pincus, R., Ploshay, J. J., Ramaswamy, V., Seman, C. J., Shevliakova, E., Sirutis, J. J., Stern, W. F., Stouffer, R. J., Wilson, R. J., Winton, M., Wittenberg, A. T., and Zeng, F.: The Dynamical Core, Physical Parameterizations, and Basic Simulation Characteristics of the Atmospheric Component AM3 of the GFDL Global Coupled Model CM3, *Journal of Climate*, 24, 3484 – 3519, <https://doi.org/10.1175/2011JCLI3955.1>, 2011.
- 190 195 Döscher, R., Acosta, M., Alessandri, A., Anthoni, P., Arsouze, T., Bergman, T., Bernardello, R., Boussetta, S., Caron, L.-P., Carver, G., Castrillo, M., Catalano, F., Cvijanovic, I., Davini, P., Dekker, E., Doblas-Reyes, F. J., Docquier, D., Echevarria, P., Fladrich, U., Fuentes-Franco, R., Gröger, M., v. Hardenberg, J., Hieronymus, J., Karami, M. P., Keskinen, J.-P., Koenigk, T., Makkonen, R., Massonnet, F., Ménégoz, M., Miller, P. A., Moreno-Chamarro, E., Nieradzik, L., van Noije, T., Nolan, P., O'Donnell, D., Ollinaho, P., van den Oord, G., Ortega, P., Prims, O. T., Ramos, A., Reerink, T., Rousset, C., Ruprich-Robert, Y., Le Sager, P., Schmitt, T., Schrödner, R., Serva, F., Sicardi, V., Sloth Madsen, M., Smith, B., Tian, T., Tourigny, E., Uotila, P., Vancoppenolle, M., Wang, S., Wårldin, D., Willén, U., Wyser, K., Yang, S., Yepes-Arbós, X., and Zhang, Q.: The EC-Earth3 Earth system model for the Coupled Model Intercomparison Project 6, *Geoscientific Model Development*, 15, 2973–3020, <https://doi.org/10.5194/gmd-15-2973-2022>, 2022.
- 200 205 Dufresne, J.-L., Foujols, M.-A., Denvil, S., Caubel, A., Marti, O., Aumont, O., Balkanski, Y., Bekki, S., Bellenger, H., Benshila, R., Bony, S., Bopp, L., Braconnot, P., Brockmann, P., Cadule, P., Cheruy, F., Codron, F., Cozic, A., Cugnet, D., de Noblet, N., Duvel, J.-P., Ethé, C., Fairhead, L., Fichefet, T., Flavoni, S., Friedlingstein, P., Grandpeix, J.-Y., Guez, L., Guilyardi, E., Hauglustaine, D., Hourdin, F., Idelkadi, A., Ghattas, J., Joussaume, S., Kageyama, M., Krinner, G., Labetoulle, S., Lahellec, A., Lefebvre, M.-P., Lefevre, F., Levy, C., Li, Z. X.,

Lloyd, J., Lott, F., Madec, G., Mancip, M., Marchand, M., Masson, S., Meurdesoif, Y., Mignot, J., Musat, I., Parouty, S., Polcher, J., Rio, C., Schulz, M., Swingedouw, D., Szopa, S., Talandier, C., Terray, P., Viovy, N., and Vuichard, N.: Climate change projections using the IPSL-CM5 Earth System Model: from CMIP3 to CMIP5, *Clim Dyn*, 40, 2123–2165, <https://doi.org/10.1007/s00382-012-1636-1>, 2013.

210 Dunne, J. P., John, J. G., Adcroft, A. J., Griffies, S. M., Hallberg, R. W., Shevliakova, E., Stouffer, R. J., Cooke, W., Dunne, K. A., Harrison, M. J., Krasting, J. P., Malyshev, S. L., Milly, P. C. D., Phillipps, P. J., Sentman, L. T., Samuels, B. L., Spelman, M. J., Winton, M., Wittenberg, A. T., and Zadeh, N.: GFDL's ESM2 Global Coupled Climate–Carbon Earth System Models. Part I: Physical Formulation and Baseline Simulation Characteristics, *Journal of Climate*, 25, 6646 – 6665, <https://doi.org/10.1175/JCLI-D-11-00560.1>, 2012.

Dunne, J. P., Horowitz, L. W., Adcroft, A. J., Ginoux, P., Held, I. M., John, J. G., Krasting, J. P., Malyshev, S., Naik, V., Paulot, F., Shevliakova, E., Stock, C. A., Zadeh, N., Balaji, V., Blanton, C., Dunne, K. A., Dupuis, C., Durachta, J., Dussin, R., Gauthier, P. P. G., Griffies, S. M., Guo, H., Hallberg, R. W., Harrison, M., He, J., Hurlin, W., McHugh, C., Menzel, R., Milly, P. C. D., Nikonorov, S., Paynter, D. J., Poshay, J., Radhakrishnan, A., Rand, K., Reichl, B. G., Robinson, T., Schwarzkopf, D. M., Sentman, L. T., Underwood, S., Vahlenkamp, H., Winton, M., Wittenberg, A. T., Wyman, B., Zeng, Y., and Zhao, M.: The GFDL Earth System Model Version 4.1 (GFDL-ESM 4.1): Overall Coupled Model Description and Simulation Characteristics, *Journal of Advances in Modeling Earth Systems*, 12, e2019MS002015, <https://doi.org/10.1029/2019MS002015>, 2020.

Flynn, C. M. and Mauritsen, T.: On the climate sensitivity and historical warming evolution in recent coupled model ensembles, *Atmospheric Chemistry and Physics*, 20, 7829–7842, <https://doi.org/10.5194/acp-20-7829-2020>, 2020.

Gent, P. R., Danabasoglu, G., Donner, L. J., Holland, M. M., Hunke, E. C., Jayne, S. R., Lawrence, D. M., Neale, R. B., Rasch, P. J., Vertenstein, M., Worley, P. H., Yang, Z.-L., and Zhang, M.: The Community Climate System Model Version 4, *Journal of Climate*, 24, 4973 – 4991, <https://doi.org/10.1175/2011JCLI4083.1>, 2011.

225 Giorgetta, M. A., Jungclaus, J., Reick, C. H., Legutke, S., Bader, J., Böttinger, M., Brovkin, V., Crueger, T., Esch, M., Fieg, K., Glushak, K., Gayler, V., Haak, H., Hollweg, H.-D., Ilyina, T., Kinne, S., Kornblueh, L., Matei, D., Mauritsen, T., Mikolajewicz, U., Mueller, W., Notz, D., Pithan, F., Raddatz, T., Rast, S., Redler, R., Roeckner, E., Schmidt, H., Schnur, R., Segschneider, J., Six, K. D., Stockhausen, M., Timmreck, C., Wegner, J., Widmann, H., Wieners, K.-H., Claussen, M., Marotzke, J., and Stevens, B.: Climate and carbon cycle changes from 1850 to 2100 in MPI-ESM simulations for the Coupled Model Intercomparison Project phase 5, *Journal of Advances in Modeling Earth Systems*, 5, 572–597, <https://doi.org/10.1002/jame.20038>, 2013.

Golaz, J.-C., Caldwell, P. M., Van Roekel, L. P., Petersen, M. R., Tang, Q., Wolfe, J. D., Abeshu, G., Anantharaj, V., Asay-Davis, X. S., Bader, D. C., Baldwin, S. A., Bisht, G., Bogenschutz, P. A., Branstetter, M., Brunke, M. A., Brus, S. R., Burrows, S. M., Cameron-Smith, P. J., Donahue, A. S., Deakin, M., Easter, R. C., Evans, K. J., Feng, Y., Flanner, M., Foucar, J. G., Fyke, J. G., Griffin, B. M., Hannay, C., Harrop, B. E., Hoffman, M. J., Hunke, E. C., Jacob, R. L., Jacobsen, D. W., Jeffery, N., Jones, P. W., Keen, N. D., Klein, S. A., Larson, V. E., Leung, L. R., Li, H.-Y., Lin, W., Lipscomb, W. H., Ma, P.-L., Mahajan, S., Maltrud, M. E., Mametjanov, A., McClean, J. L., McCoy, R. B., Neale, R. B., Price, S. F., Qian, Y., Rasch, P. J., Reeves Eyre, J. E. J., Riley, W. J., Ringler, T. D., Roberts, A. F., Roesler, E. L., Salinger, A. G., Shaheen, Z., Shi, X., Singh, B., Tang, J., Taylor, M. A., Thornton, P. E., Turner, A. K., Veneziani, M., Wan, H., Wang, H., Wang, S., Williams, D. N., Wolfram, P. J., Worley, P. H., Xie, S., Yang, Y., Yoon, J.-H., Zelinka, M. D., Zender, C. S., Zeng, X., Zhang, C., Zhang, K., Zhang, Y., Zheng, X., Zhou, T., and Zhu, Q.: The DOE E3SM Coupled Model Version 1: Overview and Evaluation at Standard Resolution, *Journal of Advances in Modeling Earth Systems*, 11, 2089–2129, <https://doi.org/10.1029/2018MS001603>, 2019.

Gregory, J. M., Ingram, W. J., Palmer, M. A., Jones, G. S., Stott, P. A., Thorpe, R. B., Lowe, J. A., Johns, T. C., and Williams, K. D.: A new method for diagnosing radiative forcing and climate sensitivity, *Geophysical Research Letters*, 31, <https://doi.org/10.1029/2003GL018747>, 2004.

- 245 Hajima, T., Watanabe, M., Yamamoto, A., Tatebe, H., Noguchi, M. A., Abe, M., Ohgaito, R., Ito, A., Yamazaki, D., Okajima, H., Ito, A.,
Takata, K., Ogochi, K., Watanabe, S., and Kawamiya, M.: Development of the MIROC-ES2L Earth system model and the evaluation of
biogeochemical processes and feedbacks, *Geoscientific Model Development*, 13, 2197–2244, <https://doi.org/10.5194/gmd-13-2197-2020>,
2020.
- 250 Hazeleger, W., Wang, X., Severijns, C., Štefănescu, S., Bintanja, R., Sterl, A., Wyser, K., Semmler, T., Yang, S., van den Hurk, B., van Noije,
T., van der Linden, E., and van der Wiel, K.: EC-Earth V2.2: description and validation of a new seamless earth system prediction model,
Clim Dyn, 39, 2611–2629, <https://doi.org/10.1007/s00382-011-1228-5>, 2012.
- He, B., Bao, Q., Wang, X., Zhou, L., Wu, X., Liu, Y., Wu, G., Chen, K., He, S., Hu, W., Li, J., Li, J., Nian, G., Wang, L., Yang, J., Zhang,
M., and Zhang, X.: CAS FGOALS-f3-L Model Datasets for CMIP6 Historical Atmospheric Model Intercomparison Project Simulation,
Adv. Atmos. Sci., 36, 771–778, <https://doi.org/10.1007/s00376-019-9027-8>, 2019.
- 255 Held, I. M., Guo, H., Adcroft, A., Dunne, J. P., Horowitz, L. W., Krasting, J., Shevliakova, E., Winton, M., Zhao, M., Bushuk, M., Wittenberg,
A. T., Wyman, B., Xiang, B., Zhang, R., Anderson, W., Balaji, V., Donner, L., Dunne, K., Durachta, J., Gauthier, P. P. G., Ginoux, P., Golaz,
J.-C., Griffies, S. M., Hallberg, R., Harris, L., Harrison, M., Hurlin, W., John, J., Lin, P., Lin, S.-J., Malyshev, S., Menzel, R., Milly, P. C. D.,
Ming, Y., Naik, V., Paynter, D., Paulot, F., Ramaswamy, V., Reichl, B., Robinson, T., Rosati, A., Seman, C., Silvers, L. G., Underwood,
S., and Zadeh, N.: Structure and Performance of GFDL's CM4.0 Climate Model, *Journal of Advances in Modeling Earth Systems*, 11,
260 3691–3727, <https://doi.org/10.1029/2019MS001829>, 2019.
- Iturbide, M., Gutiérrez, J. M., Alves, L. M., Bedia, J., Cerezo-Mota, R., Cimadevilla, E., Cofiño, A. S., Di Luca, A., Faria, S. H., Gorodetskaya,
I. V., Hauser, M., Herrera, S., Hennessy, K., Hewitt, H. T., Jones, R. G., Krakovska, S., Manzanas, R., Martínez-Castro, D.,
Narisma, G. T., Nurhati, I. S., Pinto, I., Seneviratne, S. I., van den Hurk, B., and Vera, C. S.: An update of IPCC climate reference
265 regions for subcontinental analysis of climate model data: definition and aggregated datasets, *Earth System Science Data*, 12, 2959–2970,
<https://doi.org/10.5194/essd-12-2959-2020>, 2020.
- Jeffrey, S., Rotstayn, L., Collier, M., Dravitzki, S., Hamalainen, C., Moeseneder, C., Wong, K., and Syktus, J.: Australia's CMIP5 submission
using the CSIRO-Mk3.6 model, *Australian Meteorological and Oceanographic Journal*, 63, 1–13, <https://doi.org/10.22499/2.6301.001>,
2013.
- Ji, D., Wang, L., Feng, J., Wu, Q., Cheng, H., Zhang, Q., Yang, J., Dong, W., Dai, Y., Gong, D., Zhang, R.-H., Wang, X., Liu, J., Moore,
270 J. C., Chen, D., and Zhou, M.: Description and basic evaluation of Beijing Normal University Earth System Model (BNU-ESM) version
1, *Geoscientific Model Development*, 7, 2039–2064, <https://doi.org/10.5194/gmd-7-2039-2014>, 2014.
- Jones, C. D., Hughes, J. K., Bellouin, N., Hardiman, S. C., Jones, G. S., Knight, J., Liddicoat, S., O'Connor, F. M., Andres, R. J., Bell, C.,
Boo, K.-O., Bozzo, A., Butchart, N., Cadule, P., Corbin, K. D., Doutriaux-Boucher, M., Friedlingstein, P., Gornall, J., Gray, L., Halloran,
P. R., Hurtt, G., Ingram, W. J., Lamarque, J.-F., Law, R. M., Meinshausen, M., Osprey, S., Palin, E. J., Parsons Chini, L., Raddatz, T.,
275 Sanderson, M. G., Sellar, A. A., Schurer, A., Valdes, P., Wood, N., Woodward, S., Yoshioka, M., and Zerroukat, M.: The HadGEM2-ES
implementation of CMIP5 centennial simulations, *Geoscientific Model Development*, 4, 543–570, <https://doi.org/10.5194/gmd-4-543-2011>, 2011.
- Katsavounidis, I., Jay Kuo, C.-C., and Zhang, Z.: A new initialization technique for generalized Lloyd iteration, *IEEE Signal Processing
Letters*, 1, 144–146, <https://doi.org/10.1109/97.329844>, 1994.
- 280 Kelley, M., Schmidt, G. A., Nazarenko, L. S., Bauer, S. E., Ruedy, R., Russell, G. L., Ackerman, A. S., Aleinov, I., Bauer, M., Bleck, R.,
Canuto, V., Cesana, G., Cheng, Y., Clune, T. L., Cook, B. I., Cruz, C. A., Del Genio, A. D., Elsaesser, G. S., Faluvegi, G., Kiang, N. Y.,
Kim, D., Lacis, A. A., Leboissetier, A., LeGrande, A. N., Lo, K. K., Marshall, J., Matthews, E. E., McDermid, S., Mezuman, K., Miller,

R. L., Murray, L. T., Oinas, V., Orbe, C., García-Pando, C. P., Perlwitz, J. P., Puma, M. J., Rind, D., Romanou, A., Shindell, D. T., Sun, S., Tausnev, N., Tsigaridis, K., Tselioudis, G., Weng, E., Wu, J., and Yao, M.-S.: GISS-E2.1: Configurations and Climatology, *Journal of Advances in Modeling Earth Systems*, 12, e2019MS002 025, <https://doi.org/10.1029/2019MS002025>, 2020.

285 Kuhlbrodt, T., Jones, C. G., Sellar, A., Storkey, D., Blockley, E., Stringer, M., Hill, R., Graham, T., Ridley, J., Blaker, A., Calvert, D., Copsey, D., Ellis, R., Hewitt, H., Hyder, P., Ineson, S., Mulcahy, J., Siahaan, A., and Walton, J.: The low-resolution version of HadGEM3 GC3.1: Development and evaluation for global climate, *Journal of Advances in Modeling Earth Systems*, 10, 2865–2888, <https://doi.org/10.1029/2018MS001370>, 2018.

290 Lee, J., Kim, J., Sun, M. A., Kim, B. H., Moon, H., Sung, H. M., Kim, J., and Byun, Y. H.: Evaluation of the Korea Meteorological Administration Advanced Community Earth-System model (K-ACE), *Asia-Pac J Atmos Sci*, 56, 381–395, <https://doi.org/10.1007/s13143-019-00144-7>, 2020a.

295 Lee, W.-L., Wang, Y.-C., Shiu, C.-J., Tsai, I., Tu, C.-Y., Lan, Y.-Y., Chen, J.-P., Pan, H.-L., and Hsu, H.-H.: Taiwan Earth System Model Version 1: description and evaluation of mean state, *Geoscientific Model Development*, 13, 3887–3904, <https://doi.org/10.5194/gmd-13-3887-2020>, 2020b.

Li, L., Lin, P., Yu, Y., Wang, B., Zhou, T., Liu, L., Liu, J., Bao, Q., Xu, S., Huang, W., Xia, K., Pu, Y., Dong, L., Shen, S., Liu, Y., Hu, N., Liu, M., Sun, W., Shi, X., Zheng, W., Wu, B., Song, M., Liu, H., Zhang, X., Wu, G., Xue, W., Huang, X., Yang, G., Song, Z., and Qiao, F.: The flexible global ocean-atmosphere-land system model, Grid-point Version 2: FGOALS-g2, *Adv. Atmos. Sci.*, 30, 543–560, <https://doi.org/10.1007/s00376-012-2140-6>, 2013.

300 Lovato, T., Peano, D., Butenschön, M., Materia, S., Iovino, D., Scoccimarro, E., Fogli, P. G., Cherchi, A., Bellucci, A., Gualdi, S., Masina, S., and Navarra, A.: CMIP6 Simulations With the CMCC Earth System Model (CMCC-ESM2), *Journal of Advances in Modeling Earth Systems*, 14, e2021MS002 814, [https://doi.org/https://doi.org/10.1029/2021MS002814](https://doi.org/10.1029/2021MS002814), 2022.

305 Mauritzen, T., Bader, J., Becker, T., Behrens, J., Bittner, M., Brokopf, R., Brovkin, V., Claussen, M., Crueger, T., Esch, M., Fast, I., Fiedler, S., Fläschner, D., Gayler, V., Giorgetta, M., Goll, D. S., Haak, H., Hagemann, S., Hedemann, C., Hohenegger, C., Ilyina, T., Jahns, T., Jiménez-de-la Cuesta, D., Jungclaus, J., Kleinen, T., Kloster, S., Kracher, D., Kinne, S., Kleberg, D., Lasslop, G., Kornblueh, L., Marotzke, J., Matei, D., Meraner, K., Mikolajewicz, U., Modali, K., Möbis, B., Müller, W. A., Nabel, J. E. M. S., Nam, C. C. W., Notz, D., Nyawira, S.-S., Paulsen, H., Peters, K., Pincus, R., Pohlmann, H., Pongratz, J., Popp, M., Raddatz, T. J., Rast, S., Redler, R., Reick, C. H., Rohrschneider, T., Schemann, V., Schmidt, H., Schnur, R., Schulzweida, U., Six, K. D., Stein, L., Stemmler, I., Stevens, B., von Storch, J.-S., Tian, F., Voigt, A., Vreese, P., Wieners, K.-H., Wilkenskjeld, S., Winkler, A., and Roeckner, E.: Developments in the MPI-M Earth System Model version 1.2 (MPI-ESM1.2) and Its Response to Increasing CO₂, *Journal of Advances in Modeling Earth Systems*, 11, 998–1038, <https://doi.org/10.1029/2018MS001400>, 2019.

Meehl, G., Senior, C., Eyring, V., Flato, G., Lamarque, J., Stouffer, R., Taylor, K., and Schlund, M.: Context for interpreting equilibrium climate sensitivity and transient climate response from the CMIP6 Earth system models, *Sci Adv.*, 6, eaba1981, <https://doi.org/10.1126/sciadv.aba1981>, 2020.

315 Meehl, G. A., Washington, W. M., Arblaster, J. M., Hu, A., Teng, H., Kay, J. E., Gettelman, A., Lawrence, D. M., Sanderson, B. M., and Strand, W. G.: Climate Change Projections in CESM1(CAM5) Compared to CCSM4, *Journal of Climate*, 26, 6287 – 6308, <https://doi.org/10.1175/JCLI-D-12-00572.1>, 2013.

Müller, W. A., Jungclaus, J. H., Mauritzen, T., Baehr, J., Bittner, M., Budich, R., Bunzel, F., Esch, M., Ghosh, R., Haak, H., Ilyina, T., Kleine, T., Kornblueh, L., Li, H., Modali, K., Notz, D., Pohlmann, H., Roeckner, E., Stemmler, I., Tian, F., and Marotzke, J.: A Higher-

- 320 resolution Version of the Max Planck Institute Earth System Model (MPI-ESM1.2-HR), *Journal of Advances in Modeling Earth Systems*, 10, 1383–1413, <https://doi.org/10.1029/2017MS001217>, 2018.
- Nijssse, F., Cox, P., and Williamson, M.: Emergent constraints on transient climate response (TCR) and equilibrium climate sensitivity (ECS) from historical warming in CMIP5 and CMIP6 models, *Earth System Dynamics*, 11, 737–750, <https://doi.org/10.5194/esd-11-737-2020>, 2020.
- 325 Pak, G., Noh, Y., Lee, M., Yeh, S., Kim, D., Kim, S., Lee, J., Lee, H., Hyun, S., Lee, K., Lee, J., Park, Y., Jin, H., Park, H., and Kim, Y.: Korea Institute of Ocean Science and Technology Earth System Model and Its Simulation Characteristics, *Ocean Science Journal*, 56, 18–45, <https://doi.org/10.1007/s12601-021-00001-7>, 2021.
- Pu, Y., Liu, H., Yan, R., Yang, H., Xia, K., Li, Y., Dong, L., Li, L., Wang, H., Nie, Y., Song, M., Xie, J., Zhao, S., Chen, K., Wang, B., Li, J., and Zuo, L.: CAS FGOALS-g3 Model Datasets for the CMIP6 Scenario Model Intercomparison Project (ScenarioMIP), *Adv. Atmos. Sci.*, 37, 1081–1092, <https://doi.org/10.1007/s00376-020-2032-0>, 2020.
- Schlund, M., Lauer, A., Gentine, P., Sherwood, S. C., and Eyring, V.: Emergent constraints on equilibrium climate sensitivity in CMIP5: do they hold for CMIP6?, *Earth System Dynamics*, 11, 1233–1258, <https://doi.org/10.5194/esd-11-1233-2020>, 2020.
- Schmidt, G. A., Kelley, M., Nazarenko, L., Ruedy, R., Russell, G. L., Aleinov, I., Bauer, M., Bauer, S. E., Bhat, M. K., Bleck, R., Canuto, V., Chen, Y.-H., Cheng, Y., Clune, T. L., Del Genio, A., de Fainchtein, R., Faluvegi, G., Hansen, J. E., Healy, R. J., Kiang, N. Y., Koch, D., Lacis, A. A., LeGrande, A. N., Lerner, J., Lo, K. K., Matthews, E. E., Menon, S., Miller, R. L., Oinas, V., Oloso, A. O., Perlitz, J. P., Puma, M. J., Putman, W. M., Rind, D., Romanou, A., Sato, M., Shindell, D. T., Sun, S., Syed, R. A., Tausnev, N., Tsigaridis, K., Unger, N., Voulgarakis, A., Yao, M.-S., and Zhang, J.: Configuration and assessment of the GISS ModelE2 contributions to the CMIP5 archive, *Journal of Advances in Modeling Earth Systems*, 6, 141–184, <https://doi.org/10.1002/2013MS000265>, 2014.
- Séférian, R., Nabat, P., Michou, M., Saint-Martin, D., Volodire, A., Colin, J., Decharme, B., Delire, C., Berthet, S., Chevallier, M., Sénési, S., Franchisteguy, L., Vial, J., Mallet, M., Joetzjer, E., Geoffroy, O., Guérémy, J.-F., Moine, M.-P., Msadek, R., Ribes, A., Rocher, M., Roehrig, R., Salas-y Méria, D., Sanchez, E., Terray, L., Valcke, S., Waldman, R., Aumont, O., Bopp, L., Deshayes, J., Éthé, C., and Madec, G.: Evaluation of CNRM Earth System Model, CNRM-ESM2-1: Role of Earth System Processes in Present-Day and Future Climate, *Journal of Advances in Modeling Earth Systems*, 11, 4182–4227, <https://doi.org/10.1029/2019MS001791>, 2019.
- 340 Seland, Ø., Bentsen, M., Graff, L., Olivié, D., Toniazzo, T., Gjermundsen, A., Debernard, J., Gupta, A., He, Y., Kirkevåg, A., Schwinger, J., Tjiputra, J., Aas, K., Bethke, I., Fan, Y., Griesfeller, J., Grini, A., Guo, C., Ilicak, M., and Michael, S.: The Norwegian Earth System Model, NorESM2 – Evaluation of the CMIP6 DECK and historical simulations, <https://doi.org/10.5194/gmd-2019-378>, 2020a.
- 345 Seland, Ø., Bentsen, M., Olivié, D., Toniazzo, T., Gjermundsen, A., Graff, L. S., Debernard, J. B., Gupta, A. K., He, Y.-C., Kirkevåg, A., Schwinger, J., Tjiputra, J., Aas, K. S., Bethke, I., Fan, Y., Griesfeller, J., Grini, A., Guo, C., Ilicak, M., Karset, I. H. H., Landgren, O., Liakka, J., Moseid, K. O., Nummelin, A., Spensberger, C., Tang, H., Zhang, Z., Heinze, C., Iversen, T., and Schulz, M.: Overview of the Norwegian Earth System Model (NorESM2) and key climate response of CMIP6 DECK, historical, and scenario simulations, *Geoscientific Model Development*, 13, 6165–6200, <https://doi.org/10.5194/gmd-13-6165-2020>, 2020b.
- Sellar, A. A., Jones, C. G., Mulcahy, J. P., Tang, Y., Yool, A., Wiltshire, A., O'Connor, F. M., Stringer, M., Hill, R., Palmieri, J., Woodward, S., de Mora, L., Kuhlbrodt, T., Rumbold, S. T., Kelley, D. I., Ellis, R., Johnson, C. E., Walton, J., Abraham, N. L., Andrews, M. B., Andrews, T., Archibald, A. T., Berthou, S., Burke, E., Blockley, E., Carslaw, K., Dalvi, M., Edwards, J., Folberth, G. A., Gedney, N., Griffiths, P. T., Harper, A. B., Hendry, M. A., Hewitt, A. J., Johnson, B., Jones, A., Jones, C. D., Keeble, J., Liddicoat, S., Morgenstern, O., Parker, R. J., Predoi, V., Robertson, E., Siahaan, A., Smith, R. S., Swaminathan, R., Woodhouse, M. T., Zeng, G., and Zerroukat, M.:

- UKESM1: Description and Evaluation of the U.K. Earth System Model, *Journal of Advances in Modeling Earth Systems*, 11, 4513–4558, <https://doi.org/10.1029/2019MS001739>, 2019.
- Semmler, T., Danilov, S., Gierz, P., Goessling, H. F., Hegewald, J., Hinrichs, C., Koldunov, N., Khosravi, N., Mu, L., Rackow, T., Sein, D. V., Sidorenko, D., Wang, Q., and Jung, T.: Simulations for CMIP6 With the AWI Climate Model AWI-CM-1-1, *Journal of Advances in Modeling Earth Systems*, 12, e2019MS002 009, <https://doi.org/10.1029/2019MS002009>, 2020.
- Smith, C., Nicholls, Z. R. J., Armour, K., Collins, W., Forster, P., Meinshausen, M., Palmer, M. D., and Watanabe, M.: The Earth's Energy Budget, Climate Feedbacks, and Climate Sensitivity Supplementary Material, chap. 7, <https://ipcc.ch/static/ar6/wg1>, [Masson-Delmotte, V., P. Zhai, A. Pirani, S. L. Connors, C. Péan, S. Berger, N. Caud, Y. Chen, L. Goldfarb, M. I. Gomis, M. Huang, K. Leitzell, E. Lonnoy, J.B.R. Matthews, T. K. Maycock, T. Waterfield, O. Yelekçi, R. Yu, and B. Zhou (eds.)], 2021.
- Stouffer, R.: U of Arizona MCM-UA-1-0 model output prepared for CMIP6 CMIP, <https://doi.org/10.22033/ESGF/CMIP6.2421>, 2019.
- Swart, N. C., Cole, J. N. S., Kharin, V. V., Lazare, M., Scinocca, J. F., Gillett, N. P., Anstey, J., Arora, V., Christian, J. R., Hanna, S., Jiao, Y., Lee, W. G., Majaess, F., Saenko, O. A., Seiler, C., Seinen, C., Shao, A., Sigmond, M., Solheim, L., von Salzen, K., Yang, D., and Winter, B.: The Canadian Earth System Model version 5 (CanESM5.0.3), *Geoscientific Model Development*, 12, 4823–4873, <https://doi.org/10.5194/gmd-12-4823-2019>, 2019.
- Tatebe, H., Ogura, T., Nitta, T., Komuro, Y., Ogochi, K., Takemura, T., Sudo, K., Sekiguchi, M., Abe, M., Saito, F., Chikira, M., Watanabe, S., Mori, M., Hirota, N., Kawatani, Y., Mochizuki, T., Yoshimura, K., Takata, K., O'ishi, R., Yamazaki, D., Suzuki, T., Kurogi, M., Kataoka, T., Watanabe, M., and Kimoto, M.: Description and basic evaluation of simulated mean state, internal variability, and climate sensitivity in MIROC6, *Geoscientific Model Development*, 12, 2727–2765, <https://doi.org/10.5194/gmd-12-2727-2019>, 2019.
- Tokarska, K. B., Stolpe, M. B., Sippel, S., Fischer, E. M., Smith, C. J., Lehner, F., and Knutti, R.: Past warming trend constrains future warming in CMIP6 models, *Science Advances*, 6, eaaz9549, <https://doi.org/10.1126/sciadv.aaz9549>, 2020.
- Voldoire, A., Sanchez-Gomez, E., Salas y Mélia, D., Decharme, B., Cassou, C., Sénési, S., Valcke, S., Beau, I., Alias, A., Chevallier, M., Déqué, M., Deshayes, J., Douville, H., Fernandez, E., Madec, G., Maisonnave, E., Moine, M.-P., Planton, S., Saint-Martin, D., Szopa, S., Tytca, S., Alkama, R., Belamari, S., Braun, A., Coquart, L., and Chauvin, F.: The CNRM-CM5.1 global climate model: description and basic evaluation, *Clim Dyn*, 40, 2091–2121, <https://doi.org/10.1007/s00382-011-1259-y>, 2013.
- Voldoire, A., Saint-Martin, D., Sénési, S., Decharme, B., Alias, A., Chevallier, M., Colin, J., Guérémy, J.-F., Michou, M., Moine, M.-P., Nabat, P., Roehrig, R., Salas y Mélia, D., Séférian, R., Valcke, S., Beau, I., Belamari, S., Berthet, S., Cassou, C., Cattiaux, J., Deshayes, J., Douville, H., Ethé, C., Franchistéguy, L., Geoffroy, O., Lévy, C., Madec, G., Meurdesoif, Y., Msadek, R., Ribes, A., Sanchez-Gomez, E., Terray, L., and Waldman, R.: Evaluation of CMIP6 DECK Experiments With CNRM-CM6-1, *Journal of Advances in Modeling Earth Systems*, 11, 2177–2213, <https://doi.org/10.1029/2019MS001683>, 2019.
- Volodin, E. and Gritsun, A.: Simulation of observed climate changes in 1850–2014 with climate model INM-CM5, *Earth Syst. Dynam.*, 9, 1235–1242, <https://doi.org/10.5194/esd-9-1235-2018>, 2018.
- Volodin, E., Dianskii, N., and Gusev, A.: Simulating present-day climate with the INMCM4.0 coupled model of the atmospheric and oceanic general circulations, *Izv. Atmos. Ocean. Phys.*, 46, 414–431, <https://doi.org/10.1134/S000143381004002X>, 2010.
- Volodin, E., Mortikov, E., Kostrykin, S., Galin, V., Lykossov, V., Gritsun, A., Diansky, N., Gusev, A., Iakovlev, N., Shestakova, A., and Emelina, S.: Simulation of the modern climate using the INM-CM48 climate model, *Russian Journal of Numerical Analysis and Mathematical Modelling*, 33, 367–374, 2018.

- von Salzen, K., Scinocca, J. F., McFarlane, N. A., Li, J., Cole, J. N. S., Plummer, D., Verseghy, D., Reader, M. C., Ma, X., Lazare, M., and Solheim, L.: The Canadian Fourth Generation Atmospheric Global Climate Model (CanAM4). Part I: Representation of Physical
395 Processes, *Atmosphere-Ocean*, 51, 104–125, <https://doi.org/10.1080/07055900.2012.755610>, 2013.
- Watanabe, M., Suzuki, T., O’ishi, R., Komuro, Y., Watanabe, S., Emori, S., Takemura, T., Chikira, M., Ogura, T., Sekiguchi, M., Takata, K., Yamazaki, D., Yokohata, T., Nozawa, T., Hasumi, H., Tatebe, H., and Kimoto, M.: Improved Climate Simulation by MIROC5: Mean States, Variability, and Climate Sensitivity, *Journal of Climate*, 23, 6312 – 6335, <https://doi.org/10.1175/2010JCLI3679.1>, 2010.
- Watanabe, S., Hajima, T., Sudo, K., Nagashima, T., Takemura, T., Okajima, H., Nozawa, T., Kawase, H., Abe, M., Yokohata, T., Ise, T.,
400 Sato, H., Kato, E., Takata, K., Emori, S., and Kawamiya, M.: MIROC-ESM 2010: model description and basic results of CMIP5-20c3m experiments, *Geoscientific Model Development*, 4, 845–872, <https://doi.org/10.5194/gmd-4-845-2011>, 2011.
- Wu, T., Song, L., Li, W., Wang, Z., Zhang, H., Xin, X., Zhang, Y., Zhang, L., Li, J., Wu, F., Liu, Y., Zhang, F., Shi, X., Chu, M., Zhang, J., Fang, Y., Wang, F., Lu, Y., Liu, X., Wei, M., Liu, Q., Zhou, W., Dong, M., Zhao, Q., Ji, J., Li, L., and Zhou, M.: An overview of BCC climate system model development and application for climate change studies, *Acta Meteorol Sin*, 28, 34–56, <https://doi.org/10.1007/s13351-014-3041-7>, 2014.
- Wyser, K., van Noije, T., Yang, S., von Hardenberg, J., O’Donnell, D., and Döscher, R.: On the increased climate sensitivity in the EC-Earth model from CMIP5 to CMIP6, *Geoscientific Model Development*, 13, 3465–3474, <https://doi.org/10.5194/gmd-13-3465-2020>, 2020.
- Yukimoto, S., Adachi, Y., Hosaka, M., Sakami, T., Yoshimura, H., Hirabara, M., Tanaka, T. Y., Shindo, E., Tsujino, H., Deushi, M., Mizuta, R., Yabu, S., Obata, A., Nakano, H., Koshiro, T., Ose, T., and Kitoh, A.: A New Global Climate Model of the Meteorological Research
410 Institute: MRI-CGCM3 mdash;Model Description and Basic Performance mdash;, *Journal of the Meteorological Society of Japan. Ser. II*, 90A, 23–64, <https://doi.org/10.2151/jmsj.2012-A02>, 2012.
- Yukimoto, S., Kawai, H., Koshiro, T., Oshima, N., Yoshida, K., Urakawa, S., Tsujino, H., Deushi, M., Tanaka, T., Hosaka, M., Yabu, S., Yoshimura, H., Shindo, E., Mizuta, R., Obata, A., Adachi, Y., and Ishii, M.: The Meteorological Research Institute Earth System Model Version 2.0, MRI-ESM2.0: Description and Basic Evaluation of the Physical Component, *Journal of the Meteorological Society of Japan. Ser. II*, 415 *advpub*, 2019–051, <https://doi.org/10.2151/jmsj.2019-051>, 2019.
- Zelinka, M. D., Myers, T. A., McCoy, D. T., Po-Chedley, S., Caldwell, P. M., Ceppi, P., Klein, S. A., and Taylor, K. E.: Causes of Higher Climate Sensitivity in CMIP6 Models, *Geophysical Research Letters*, 47, e2019GL085782, <https://doi.org/https://doi.org/10.1029/2019GL085782>, 2020.
- Zhang, H., Zhang, M., Jin, J., Fei, K., Ji, D., Wu, C., Zhu, J., He, J., Chai, Z., Xie, J., Dong, X., Zhang, D., Bi, X., Cao, H., Chen, H., Chen,
420 K., Chen, X., Gao, X., Hao, H., Jiang, J., Kong, X., Li, S., Li, Y., Lin, P., Lin, Z., Liu, H., Liu, X., Shi, Y., Song, M., Wang, H., Wang, T., Wang, X., Wang, Z., Wei, Y., Wu, B., Xie, Z., Xu, Y., Yu, Y., Yuan, L., Zeng, Q., Zeng, X., Zhao, S., Zhou, G., and Zhu, J.: Description and Climate Simulation Performance of CAS-ESM Version 2, *Journal of Advances in Modeling Earth Systems*, 12, e2020MS002210, <https://doi.org/https://doi.org/10.1029/2020MS002210>, 2020.
- Ziehn, T., Chamberlain, M. A., Law, R. M., Lenton, A., Bodman, R. W., Dix, M., Stevens, L., Wang, Y.-P., and Srbinovsky, J.:
425 The Australian Earth System Model: ACCESS-ESM1.5, *Journal of Southern Hemisphere Earth Systems Science*, 70, 193–214, <https://doi.org/https://doi.org/10.1071/ES19035>, 2020.

Table S1. Additional information about the CMIP6 multi-model ensemble used in this study (1/2). Further information on atmospheric components and nominal resolution can be found at https://wcrp-cmip.github.io/CMIP6_CVs/docs/CMIP6_source_id.html.

ID	Model Name	Atmospheric Component	Nominal Resolution	Members	Case Member(s)?	Study Reference
1)	ACCESS-ESM1-5	HadGAM2	250 km	r(1-10)i1p1f1	All	Ziehn et al. (2020)
2)	HadGEM3-GC31-MM	MetUM-HadGEM3-GA7.1	100 km	r(1-4)i1p1f3	All	Andrews et al. (2020)
3)	KACE-1-0-G	MetUM-HadGEM3-GA7.1	250 km	r(1-3)i1p1f1	r(2,3)i1p1f1	Lee et al. (2020a)
4)	ACCESS-CM2	MetUM-HadGEM3-GA7.1	250 km	r(1-3)i1p1f1	All	Bi et al. (2020)
5)	HadGEM3-GC31-LL	MetUM-HadGEM3-GA7.1	250 km	r(1-4)i1p1f3	All	Kuhlbrodt et al. (2018)
6)	UKESM1-0-LL	MetUM-HadGEM3-GA7.1	250 km	r(1-4,8)i1p1f2	All	Sellar et al. (2019)
7)	TaiESM1	TaiAM1	100 km	r1i1p1f1	Yes	Lee et al. (2020b)
8)	CMCC-ESM2	CAM5.3	100 km	r1i1p1f1	Yes	Lovato et al. (2022)
9)	CMCC-CM2-SR5	CAM5.3	100 km	r1i1p1f1	Yes	Cherchi et al. (2019)
10)	NorESM2-MM	CAM-OSLO	100 km	r1i1p1f1	Yes	Seland et al. (2020b)
11)	CESM2-WACCM	WACCM6	100 km	r(1-3)i1p1f1	All	Danabasoglu et al. (2020)
12)	CESM2	CAM6	100 km	r(1,2,4,10,11)i1p1f1	All	Danabasoglu et al. (2020)
13)	CNRM-CM6-1-HR	Arpege 6.3	100 km	r1i1p1f2	Yes	Voldoire et al. (2019)
14)	CNRM-ESM2-1	Arpege 6.3	250 km	r(1-5)i1p1f2	All	Séférian et al. (2019)
15)	IPLS-CM6A-LR	LMDZ	250 km	r(1-4,6,14)i1p1f1	All	Boucher et al. (2020)
16)	CNRM-CM6-1	Arpege 6.3	250 km	r(1-6)i1p1f2	All	Voldoire et al. (2019)
17)	AWI-CM-1-1-MR	ECHAM6.3	100 km	r1i1p1f1	Yes	Semmler et al. (2020)
18)	NESM3	ECHAM6.3	250 km	r(1,2)i1p1f1	All	Cao et al. (2018)
19)	MPI-ESM1-2-LR	ECHAM6.3	250 km	r(1-10)i1p1f1	All	Mauritsen et al. (2019)
20)	MPI-ESM1-2-HR	ECHAM6.3	100 km	r(1,2)i1p1f1	All	Müller et al. (2018)

Table S2. Summary of the CMIP6 multi-model ensemble used in this study (2/2). Further information can be found at https://wcrp-cmip.github.io/CMIP6_CVs/docs/CMIP6_source_id.html.

ID	Model Name	Atmospheric Component	Nominal Resolution	Members	Case Member(s)?	Study Reference
21)	GFDL-CM4	GFDL-AM4.0.1	100 km	r1i1p1f1	Yes	Held et al. (2019)
22)	GFDL-ESM4	GFDL-AM4.1	100 km	r1i1p1f1	Yes	Dunne et al. (2020)
23)	EC-Earth3	IFS cy36r4	100 km	r(1,3,4,6,9,11,13,15)i1p1f1	None	Dööscher et al. (2022)
24)	EC-Earth3-Veg	IFS cy36r4	100 km	r(1-4)i1p1f1	None	Dööscher et al. (2022)
25)	FGOALS-f3-L	FAMIL2.2	100 km	r1i1p1f1	Yes	He et al. (2019)
26)	FGOALS-g3	GAMIL3	250 km	r(1-4)i1p1f1	r(1,2)i1p1f1	Pu et al. (2020)
27)	INM-CM4-8	INM-AM4-8	100 km	r1i1p1f1	Yes	Volodin et al. (2018)
28)	INM-CM5-0	INM-AM5-0	100 km	r1i1p1f1	Yes	Volodin and Gritsun (2018)
29)	MIROC6	CCSR AGCM	250 km	r(1-50)i1p1f1	All	Tatebe et al. (2019)
30)	MIROC-ES2L	CCSR AGCM	500 km	r(1-10)i1p1f2	All	Hajima et al. (2020)
31)	MRI-ESM2-0	MRI-AGCM3.5	100 km	r1i(1,2)p1f1	All	Yukimoto et al. (2019)
32)	E3SM-1-1	EAM	100 km	r1i1p1f1	Yes	Golaz et al. (2019)
33)	CanESM5	CanAM5	500 km	r(1-25)i1p1(1,2)f1	Yes	Swart et al. (2019)
34)	CAS-ESM2-0	IAP AGCM 5.0	100 km	r(1,3)i1p1f1	All	Zhang et al. (2020)
35)	GISS-E2-1-G	GISS-E2.1	250 km	r(1-5)i1p3f1,r1i1p5f1	r1i1p3f1	Kelley et al. (2020)
36)	MCM-UA-1-0	R30L14	250 km	r1i1p1f2	No	Stouffer (2019)
37)	KIOST-ESM	GFDL-AM2.0	250 km	r1i1p1f1	Yes	Pak et al. (2021)

Table S3. Additional information about CMIP5 multi-model ensemble used in this study.

ID	Model Name	Atmospheric Component	Nominal Resolution	Members	Case Study Member(s)?	Reference
1)	ACCESS1-0	HadGAM2	100 km	r1i1p1	Yes	Bi et al. (2012)
2)	ACCESS1-3	UM7.3/GA1	100 km	r1i1p1	Yes	Bi et al. (2012)
3)	HadGEM2-ES	HadGAM2	100 km	r(1-4)i1p1	All	Jones et al. (2011)
4)	NorESM1-ME	CAM4-Oslo	250 km	r1i1p1	Yes	Bentsen et al. (2013)
5)	NorESM1-M	CAM4-Oslo	250 km	r1i1p1	Yes	Bentsen et al. (2013)
6)	CCSM4	CAM4	100 km	r(1-6)i1p1	All	Gent et al. (2011)
7)	CESM1-CAM5	CAM5.2	100 km	r(1-3)i1p1	All	Meehl et al. (2013)
8)	IPSL-CM5B-LR	LMDZ5B	500 km	r1i1p1	Yes	Dufresne et al. (2013)
9)	IPSL-CM5A-MR	LMDZ5A	250 km	r1i1p1	Yes	Dufresne et al. (2013)
10)	IPSL-CM5A-LR	LMDZ5A	500 km	r(1-4)i1p1	All	Dufresne et al. (2013)
11)	EC-EARTH	IFS cy31rl	250 km	r(1,2,8,9,12)i1p1	None	Hazeleger et al. (2012)
12)	CNRM-CM5	Arpege 5.2	250 km	r(1,2,4,6,10)i1p1	All	Voldoire et al. (2013)
13)	MPI-ESM-MR	ECHAM6.1	250 km	r1i1p1	Yes	Giorgetta et al. (2013)
14)	MPI-ESM-LR	ECHAM6.1	250 km	r(1-3)i1p1	All	Giorgetta et al. (2013)
15)	GFDL-ESM2G	GFDL-AM2	250 km	r1i1p1	Yes	Dunne et al. (2012)
16)	GFDL-ESM2M	GFDL-AM2	250 km	r1i1p1	Yes	Dunne et al. (2012)
17)	GFDL-CM3	GFDL-AM3	250 km	r1i1p1	Yes	Donner et al. (2011)
18)	MIROC5	CCSR-NIES-FRCGC AGCM	250 km	r(1-3)i1p1	All	Watanabe et al. (2010)
19)	MIROC-ESM	MIROC-AGCM	500 km	r1i1p1	Yes	Watanabe et al. (2011)
20)	GISS-E2-H	GISS-E2	250 km	r1i1p(1-3),r2i1p(1,3)	All	Schmidt et al. (2014)
21)	GISS-E2-R	GISS-E2	250 km	r1i1p(1-3),r2i1p(1,3)	All	Schmidt et al. (2014)
22)	bcc-csm1-1	BCC-AGCM2.1	250 km	r1i1p1	Yes	Wu et al. (2014)
23)	bcc-csm1-1-m	BCC-AGCM2.2	100 km	r1i1p1	Yes	Wu et al. (2014)
24)	BNU-ESM	CAM3.5	500 km	r1i1p1	No	Ji et al. (2014)
25)	inmcm4	INM-AM4	100 km	r1i1p1	Yes	Volodin et al. (2010)
26)	CanESM2	CanAM4	500 km	r(1-5)i1p1	All	von Salzen et al. (2013)
27)	MRI-CGCM3	MRI-AGCM3	100 km	r1i1p1	Yes	Yukimoto et al. (2012)
28)	CSIRO-Mk3-6-0	Mk3.6 AGCM	250 km	r(1-10)i1p1	All	Jeffrey et al. (2013)
29)	FGOALS-g2	GAMIL2	500 km	r1i1p1	No	Li et al. (2013)

Table S4. One member per model CMIP6 multi-model ensemble used in the between-model spread component of the model-family-defining optimal fingerprint mask.

ID	Model Name	Members	ID	Model Name	Members
1)	ACCESS-ESM1-5	r1i1p1f1	20)	MPI-ESM1-2-HR	r1i1p1f1
2)	HadGEM3-GC31-MM	r1i1p1f3	21)	GFDL-CM4	r1i1p1f1
3)	KACE-1-0-G	r1i1p1f1	22)	GFDL-ESM4	r1i1p1f1
4)	ACCESS-CM2	r1i1p1f1	23)	EC-Earth3	r1i1p1f1
5)	HadGEM3-GC31-L1	r1i1p1f3	24)	EC-Earth3-Veg	r1i1p1f1
6)	UKESM1-0-LL	r1i1p1f2	25)	FGOALS-f3-L	r1i1p1f1
7)	TaiESM1	r1i1p1f1	26)	FGOALS-g3	r1i1p1f1
8)	CMCC-ESM2	r1i1p1f1	27)	INM-CM4-8	r1i1p1f1
9)	CMCC-CM2-SR5	r1i1p1f1	28)	INM-CM5-0	r1i1p1f1
10)	NorESM2-MM	r1i1p1f1	29)	MIROC6	r1i1p1f1
11)	CESM2-WACCM	r1i1p1f1	30)	MIROC-ES2L	r1i1p1f2
12)	CESM2	r1i1p1f1	31)	MRI-ESM2-0	r1i1p1f1
13)	CNRM-CM6-1-HR	r1i1p1f2	32)	E3SM-1-1	r1i1p1f1
14)	CNRM-ESM2-1	r1i1p1f2	33)	CanESM5	r1i1p1f1
15)	IPSL-CM6A-LR	r1i1p1f1	34)	CAS-ESM2-0	r1i1p1f1
16)	CNRM-CM6-1	r1i1p1f2	35)	GISS-E2-1-G	r1i1p3f1
17)	AWI-CM-1-1-MR	r1i1p1f1	36)	MCM-UA-1-0	r1i1p1f2
18)	NESM3	r1i1p1f1	37)	KIOST-ESM	r1i1p1f1
19)	MPI-ESM1-2-LR	r1i1p1f1			

Table S5. Summary of all recommended model subsets (1/2). Each application is listed with its performance recommendation threshold. For each recommendation, the median values of α and β for the region in $\alpha\text{-}\beta$ space covered by the recommended subset are used to define the relative importance of performance, independence, and spread in the selection cost function.

CMP6 JJA CEU, 3 model subsets by Ensemble Means; Performance Rank $\geq 23/34$

Perf Ranks	Perf, Ind, Spred %	Model Names
#1, 2, 4	96%, 4%, 0%	AWI-CM-1-1-MR, HadGEM3-GC31-MM, TaiESM1
#1, 2, 5	85%, 6%, 9%	AWI-CM-1-1-MR, HadGEM3-GC31-MM, GFDL-ESM4
#1, 2, 6	88%, 10%, 2%	AWI-CM-1-1-MR, HadGEM3-GC31-MM, GFDL-CM4
#1, 5, 20	69%, 8%, 23%	AWI-CM-1-1-MR, GFDL-ESM4, UKESM1-0-LL
#5, 7, 23	71%, 14%, 15%	GFDL-ESM4, CMCC-ESM2, MIROC-ES2L
#6, 7, 23	62%, 31%, 7%	GFDL-CM4, CMCC-ESM2, MIROC-ES2L
#4, 6, 23	55%, 44%, 1%	TaiESM1, GFDL-CM4, MIROC-ES2L
#6, 13, 23	47%, 52%, 1%	GFDL-CM4, CESM2, MIROC-ES2L
#1, 7, 22	69%, 10%, 21%	AWI-CM-1-1-MR, CMCC-ESM2, CanESM5
#5, 7, 22	66%, 11%, 23%	GFDL-ESM4, CMCC-ESM2, CanESM5
#5, 20, 22	48%, 7%, 45%	GFDL-ESM4, UKESM1-0-LL, CanESM5
#2, 4, 5	71%, 11%, 18%	HadGEM3-GC31-MM, TaiESM1, GFDL-ESM4
#20, 22, 23	40%, 20%, 40%	UKESM1-0-LL, CanESM5, MIROC-ES2L
#7, 22, 23	57%, 25%, 18%	CMCC-ESM2, CanESM5, MIROC-ES2L
#13, 18, 23	36%, 60%, 4%	CESM2, IPSL-CM6A-LR, MIROC-ES2L
CMP6 JJA CEU, 3 model subsets by Individual Member; Performance Rank $\geq 23/34$		
#1, 2, 4	88%, 8%, 4%	AWI-CM-1-1-MR-r1i1p1f1, HadGEM3-GC31-MM-r1i1p1f3, MRI-ESM2-0-r1i1p1f1
#1, 2, 6	85%, 4%, 11%	AWI-CM-1-1-MR-r1i1p1f1, HadGEM3-GC31-MM-r1i1p1f3, GFDL-ESM4-r1i1p1f1
#1, 2, 20	75%, 7%, 18%	AWI-CM-1-1-MR-r1i1p1f1, HadGEM3-GC31-MM-r1i1p1f3, CanESM5-r1i1p1f1
#1, 2, 23	75%, 14%, 11%	AWI-CM-1-1-MR-r1i1p1f1, HadGEM3-GC31-MM-r1i1p1f2
#2, 3, 20	73%, 3%, 24%	HadGEM3-GC31-MM-r1i1p1f1, MPI-ESM1-2-HR-r1i1p1f1, CanESM5-r1i1p1f1
#7, 8, 23	65%, 27%, 8%	GFDL-CM4-r1i1p1f1, CMCC-ESM2-r1i1p1f1, MIROC-ES2L-r1i1p1f2
#2, 6, 20	64%, 12%, 24%	HadGEM3-GC31-MM-r1i1p1f3, GFDL-ESM4-r1i1p1f1, CanESM5-r1i1p1f1
#3, 20, 22	48%, 5%, 47%	MPI-ESM1-2-HR-r1i1p1f1, CanESM5-r1i1p1f1, UKESM1-0-LL-r1i1p1f2

Table S6. Summary of all recommended model subsets (2/2).

CMIP6 JJA CEU, 5 model subsets by Individual Member; Performance Rank $\geq 23/34$

Perf Ranks	Perf, Ind, Sprd %	Model Names
#1, 2, 4, 5, 6	92%, 4%, 4%	AWI-CM-1-1-MR-rii1p1f1, HadGEM3-GC31-MM-rii1p1f3, MRI-ESM2-0-rii1p1f1, TaiESM1-rii1p1f1, GFDL-ESM4-rii1p1f1
#1, 2, 4, 5, 7	95%, 5%, 0%	AWI-CM-1-1-MR-rii1p1f1, HadGEM3-GC31-MM-rii1p1f3, MRI-ESM2-0-rii1p1f1, TaiESM1-rii1p1f1, GFDL-CM4-rii1p1f1
#1, 2, 4, 5, 23	85%, 13%, 2%	AWI-CM-1-1-MR-rii1p1f1, HadGEM3-GC31-MM-rii1p1f3, MRI-ESM2-0-rii1p1f1, MIROC-ES2L-rii1p1f2
#1, 2, 5, 6, 23	87%, 7%, 6%	AWI-CM-1-1-MR-rii1p1f1, HadGEM3-GC31-MM-rii1p1f3, TaiESM1-rii1p1f1, GFDL-ESM4-rii1p1f1, MIROC-ES2L-rii1p1f2
#1, 2, 6, 8, 20	85%, 5%, 10%	AWI-CM-1-1-MR-rii1p1f1, HadGEM3-GC31-MM-rii1p1f3, GFDL-ESM4-rii1p1f1, CMCC-ESM2-rii1p1f1, CanESM5-r16ip1f1
#1, 6, 8, 20, 22	77%, 5%, 18%	AWI-CM-1-1-MR-rii1p1f1, GFDL-ESM4-rii1p1f1, CMCC-ESM2-rii1p1f1, CanESM5-r16ip1f1, UKESM1-0-LL-rii1p1f2
CMIP6 DJF NEU, 5 model subsets by Individual Member; Performance Rank $\geq 31/34$		
#1, 2, 7, 11, 30	67%, 26%, 7%	AWI-CM-1-1-MR-rii1p1f1, HadGEM3-GC31-MM-rii1p1f3, CNRM-CM6-1-rii1p1f2, CESM2-WACCM-rii1p1f1, MIROC-ES2L-rii1p1f2
#1, 5, 7, 11, 30	61%, 23%, 16%	AWI-CM-1-1-MR-rii1p1f1, KACE-1-0-G-rii1p1f1, CNRM-CM6-1-rii1p1f2, CESM2-WACCM-rii1p1f1, MIROC-ES2L-rii1p1f2
#1, 7, 11, 28, 30	53%, 28%, 19%	AWI-CM-1-1-MR-rii1p1f1, CNRM-CM6-1-rii1p1f2, CESM2-WACCM-rii1p1f1, E3SM-1-1-rii1p1f1, MIROC-ES2L-rii1p1f2
#7, 11, 28, 30, 31	31%, 49%, 20%	CNRM-CM6-1-rii1p1f2, CESM2-WACCM-rii1p1f1, E3SM-1-1-rii1p1f1, MIROC-ES2L-rii1p1f2, MIROC6-r12ip1f1
#2, 7, 11, 30, 31	54%, 35%, 11%	HadGEM3-GC31-MM-rii1p1f3, CNRM-CM6-1-rii1p1f2, CESM2-WACCM-rii1p1f2, MIROC-ES2L-rii1p1f2, MIROC6-r12ip1f1
CMIP5 JJA CEU, 5 model subsets by Individual Member; Performance Rank $\geq 17/26$; 3 quadrant spread		
#1, 2, 4, 5, 6	86%, 7%, 7%	GFDL-CM3-rii1p1, NorESM1-ME-rii1p1, CESM1-CAM5-rii1p1, GFDL-ESM2M-rii1p1, ACCESS1-0-rii1p1
#1, 2, 4, 5, 8	86%, 10%, 4%	GFDL-CM3-rii1p1, NorESM1-ME-rii1p1, CESM1-CAM5-rii1p1, GFDL-ESM2M-rii1p1, MIROC5-rii1p1
#1, 2, 4, 5, 10	82%, 8%, 10%	GFDL-CM3-rii1p1, NorESM1-ME-rii1p1, CESM1-CAM5-rii1p1, GFDL-ESM2M-rii1p1, HadGEM2-ES-rii1p1
#1, 2, 5, 8, 13	79%, 17%, 4%	GFDL-CM3-rii1p1, NorESM1-ME-rii1p1, GFDL-ESM2M-rii1p1, MIROC5-rii1p1, bc-csm1-1-m-rii1p1
#1, 2, 5, 10, 13	78%, 11%, 11%	GFDL-CM3-rii1p1, NorESM1-ME-rii1p1, GFDL-ESM2M-rii1p1, HadGEM2-ES-rii1p1, bc-csm1-1-n-rii1p1
#1, 2, 5, 13, 16	77%, 13%, 10%	GFDL-CM3-rii1p1, NorESM1-ME-rii1p1, GFDL-ESM2M-rii1p1, bc-csm1-1-m-rii1p1, CSIRO-Mk3-6-0-ri10ip1
CMIP5 DJF NEU, 5 model subsets by Individual Member; Performance Rank $\geq 17/26$; 3 quadrant spread		
#1, 2, 3, 5, 9	89%, 8%, 3%	ACCESS1-0-rii1p1, CESM1-CAM5-rii1p1, GFDL-CM3-rii1p1, MPI-ESM-LR-rii1p1, MIROC5-rii1p1
#1, 2, 3, 6, 9	92%, 8%, 0%	ACCESS1-0-rii1p1, CESM1-CAM5-rii1p1, GFDL-CM3-rii1p1, MPI-ESM-MR-rii1p1, MIROC5-rii1p1
#1, 2, 3, 8, 9	89%, 11%, 0%	ACCESS1-0-rii1p1, CESM1-CAM5-rii1p1, GFDL-CM3-rii1p1, GFDL-ESM2M-rii1p1, MIROC5-rii1p1
#1, 2, 3, 9, 10	84%, 14%, 2%	ACCESS1-0-rii1p1, CESM1-CAM5-rii1p1, GFDL-CM3-rii1p1, MIROC5-rii1p1, NorESM1-ME-rii1p1
#1, 2, 3, 9, 12	81%, 9%, 10%	ACCESS1-0-rii1p1, CESM1-CAM5-rii1p1, GFDL-CM3-rii1p1, MIROC5-rii1p1, GFDL-ESM2G-rii1p1
#1, 2, 8, 9, 13	83%, 17%, 0%	ACCESS1-0-rii1p1, CESM1-CAM5-rii1p1, GFDL-ESM2M-rii1p1, MIROC5-rii1p1, inmcm4-rii1p1
#1, 2, 9, 12, 14	76%, 16%, 8%	ACCESS1-0-rii1p1, CESM1-CAM5-rii1p1, GFDL-ESM2G-rii1p1, GISS-E2-R-rii1p3